SMOS L1 Processor

Table Generation Requirements Document

Code : SO-TGRD-DME-L1OP-0023
Issue : 3.12
Date : 15/12/17

	Name	Function	Signature
Prepared by	G. Lopes	Project Engineer	
	J. Barbosa	Project Engineer	
Checked by	A.Gutiérrez	Quality A. Manager	
Approved by	J. Barbosa	Project Manager	

DEIMOS Engenharia
Av. D. João II, Lote 1.17, Torre Zen, 10º
1998-023 Lisboa, PORTUGAL
Tel: +351 21 893 3013
Fax: +351 21 896 9099
E-mail: mailto:deimos@deimos.com.pt

This page intentionally left blank

Document Information

Contract Data	Classification
Contract Number: 4000101241/10/I-AM	**Internal** ☑
	Public ☐
Contract Issuer: ESA	**Industry** ☐
	Confidential ☐

Internal Distribution		
Name	Unit	Copies

External Distribution		
Name	Organisation	Copies
Manuel Martin-Neira	ESA	1
Raffaele Crapolicchio	ESA	1

Archiving	
Word Processor:	MS Word 2000
File Name:	SO-TGRD-DME-L1OP-0023_Table-Generation-Requirements-Document-E3-R11.docx
Archive Code:	SO-TGRD-DME-L1OP-0023

Document Status Log

Issue	Change description	Date	Approved
Draft	First version of the document	12-05-2006	
1.0	Version delivered for the OSAT	05-06-2006	
1.1	Version delivered after the OSAT	29-06-2006	
1.2	Updated Land/Sea Mask Auxiliary Data File. Corrected Total Size of Land/Mask and Galaxy Map ADFs for consistency.	20-07-2006	
1.3	Added ADF headers to ADF Package	26-07-2006	
1.4	Update for L1OP CDR	26-10-2006	
2.0	Update for L1PP V2R	17-11-2006	
2.1	Update for L1PP V3R	09-04-2007	
2.2	Update for L1PP V3.5R	17-07-2007	
2.3	Update for L1PP V4R	26-11-2007	
2.4	Update for L1PP V5R	04-04-2008	
2.5	Update for L1PP V6R	25-07-2008	
2.6	Update for L1PP V6.5R	22-10-2008	
2.7	Update for L1PP v3.1.0	19-05-2009	
2.8	Update for L1PP v2.2.0	24-07-2009	
2.9	Update for L1PP v3.2.0	24-09-2009	
2.10	Update for L1PP v3.3.0	26-03-2010	
2.11	Update for L1PP v3.4.0	31-05-2010	
2.12	Updated after review for the Maintenance Phase and for L1PP v3.5.0	29-10-2010	
2.13	Update for L1PP v5.0.0	20-05-2011	
2.14	Update for L1PP v5.5.0	29-11-2011	
3.0	Update for L1PP v6.0.0	30-11-2012	
	Moved contents related to AUX file generation from L1b DPM Re-versioning for L1OP contract and renamed document to reflect the new scope Changed document ID from SO-TDD-DME-L1PP-0023-ADF-set-description to SO-TGRD-DME-L1PP-0023-ADF-set-description		
3.1	First release for L1OP v600	02-05-2013	

	Changed document ID Cleaned references to L1PP and SEPS Update ADF name list		
3.2	Added Dates and versions to all Reference Documents Added changes to ADFs requested by Cal Team, in Section 4 (AUX_FAIL, AUX_LCF, AUX_NIR)	29-05-2013	
3.3	Updated information in tables 9 and 10 about BWGHT, PMS, PLM, GALAXY, GMATD and JMATD ADF updates	05-08-2013	
3.4	Updated for L1OP v6.1.0 Updated for Full Cross-Polar G usage (Section 3.1) Updated ADF list for new MISP, BFP, GALAXY and GALNIR ADFs as well as new OPER versions of remaining ADFs (Section 4)	10-09-2013	
3.5	Updated with comments at the FAT	12-09-2013	
3.6	Updated for L1OP v6.2.0 Documented changes in LCF, NIR, SPAR, GMAT, JMAT and CNF auxiliary data files	25-03-2014	
3.7	Added references for RFI list generation and BFP update Removed section on RFI detection algorithms in L1PP	09/04/2014	
3.8	Added updates to CNFL1P, LCF and PLM ADFs done to support ALL-LICEF mode and Gkj correction Detailed new way to compute Antenna Patterns averages for the ALL-LICEF G/J+	05/06/2015	
3.9	Added requested L1C RFI flagging thresholds Added FWF ADF to the list of science L1A inputs Updated the receiver phases Updated PMS Gains Sensitivities Added new product characterization parameters for the double exponential delay algorithm	02/12/2016	
3.10	Minor typos fixed, updated reference for PMS Gain Sensitivities Updated according to comments in L1OP v711 FAT	31/01/2017	
3.11	Updated for L1OP v720: Updated NIR propagation parameters and Tp7 latency parameters New Antenna Pattern Format New Configuration Flags New CAS factors Added independent Gkj factors for NIR and ALL-LICEF	28/11/2017	

	modes Added new Fresnel static map ADF		
3.12	Implemented comments received at L1OP v720 FAT: Section 3.1.2.1 – Detailed pre-processing of the antenna patterns Section 3.1.6 – corrected the text referencing the antenna patterns section Section 4 – Added separate descriptions for G/J+ for ALL-LICEF mode, added reference for new AUX_PATT data and provided more details for the applicability of the new SPAR data Section 5 – Added separate descriptions for G/J+ for ALL-LICEF mode	12/15/2017	

Table of Contents

List of Figures

List of Tables

1. INTRODUCTION

1.1. Purpose and Scope

This document describes the SMOS Level 1 Operational Processor (L1OP) Auxiliary Data Files (ADFs). The purpose of the document is not to specify the format of the files but rather to identify the files that are delivered together with the L1OP and provide a summary description of their contents[1].

As of L1OP v6.0.0, this document will also contain the description of the procedures needed to generate the ancillary files used during the L1 processing, such as the G/J+ matrices and Flat Target Transformation data.

This document is to be used by L1OP users as a support document and complements the Software User Manual Document [AD.9].

The files described in this document correspond to the baseline ADF Set 7.2.0.

1.2. Acronyms and Abbreviations

For the list of acronyms, please refer to the "Directory of Acronyms and abbreviations" [RD.1].

1.3. Applicable and Reference Documents

1.3.1. Applicable Documents

Ref.	Code	Title	Issue
AD.2	ECSS-E-40B	ECSS E-40 Software Engineering Standards	
AD.4	SO-DS-DME-L1OP-0007	SMOS L1OP DPM L1a	***2.22*** *28/11/2017*
AD.5	SO-DS-DME-L1OP-0008	SMOS L1OP DPM L1b	***2.23*** *28/11/2017*
AD.6	SO-DS-DME-L1OP-0009	SMOS L1OP DPM L1c	***2.17*** *28/11/2017*
AD.8	SO-SVVP-ST-DME-L1OP-0329	L1OP v720 Specific and System Validation and Verification Plan System Tests	***1.1*** *15/12/2017*
AD.9	SO-SUM-DME-L1OP-0278	L1OP v720 Software User Manual	***1.8*** *30/11/2017*

[1] For further information regarding the format of the files, please refer to AD13.

Ref.	Code	Title	Issue
AD.11	SO-TN-UPC-PLM-0019	SMOS In Orbit Calibration Plan Phase C-D	**1.5** *17/01/07*
AD.12	PE-TN-ESA-GS-001	Earth Explorer Ground Segment File Format Standard	**1.4**
AD.13	SO-TN-IDR-GS-0005	SMOS Level 1 and Auxiliary Data Products Specifications	**6.5** *15/12/17* *(Preliminary Version)*

Table 1-1: Applicable Documents

1.3.2. Reference Documents

Ref.	Code	Title	Issue
RD.1	SO-LI-CASA-PLM-0094	Directory of Acronyms and abbreviations	
RD.2	SO-TN-DME-L1PP-0024	SMOS L1 Full Polarisation Data Processing	**1.6** *16/07/07*
RD.3	Fernando Martin-Porqueras	Sky Visibilities Images Including Cross-polar and Polar Coordinates.pptx	**1.0** *20/08/12*
RD.4	SO-TN-UPC-PLM-0151	Antenna pattern renormalization	1.0 *28/09/12*
RD.5	SO-TN-UPC-PLM-0143	ATBD for baseline based FTT	**1.0** *29/03/12*
RD.6	SO-DS-DME-L1PP-0202	SMOS L1PP Baselines Avoidance Algorithm	**1.1** *24/07/09*
RD.7	SO-TN-UPC-PLM-0159	Review of IVT relative phases	**1.1** *25/04/13*
RD.8	SO-TN-CASA-PLM-0279_	SMOS-PLM COMMAND AND CONTROL	**2.5** *12/02/07*
RD.9	SO-TN-CASA-PLM-0594	SMOS-PLM	**3.2** *18/02/08*
RD.10	NIRC-TKK-TN-0035	Thermal coefficients of the NIR units with L1 calibration	**1.0** *20/01/12*

Ref.	Code	Title	Issue
RD.11	NIRC-TKK-TN-0023	In-Orbit Commissioning of NIR	***1.0*** *18/02/11*
RD.12	SO-TN-UPC-PLM- 0140	CAS factors independent of antenna efficiency	***1.0*** *26/0911*
RD.13	SM-TN-AURO-L1OP-0001	TN on the L1c Flags for RFI	***2.0*** *27/05/16*
RD.14	SO-TN-UPC-PLM- 0163	Front-end loss and CAS factors	***1.0*** *20/02/14*
RD.15	NIR-TN-HARP-001	NIR sensitivity to diode temperature – u-parameters for the NIR model	***1.1*** *20/02/14*
RD.16	*Eric Anterrieu (IRAP)*	RFI detection in NIR signals	***1.0*** *31/05/12*
RD.17	*Soldo, Y., Khazaal, A., Cabot, F., Anterrieu, E., & Richaume, P.*	RFI mitigation for SMOS: a distributed approach.	*IEEE Trans. on Geosci. and Remote Sens*
RD.18	*Soldo, Y., Khazaal, A., Slominska, E., Cabot, F., Fieuzal, R., Kerr, Y.H.*	Monitoring of RFI localizations for the SMOS mission: seasonal variations and systematic errors	*IEEE JSTARS*
RD.19	SMOS-CEC-VEG-IPF-REP-0609	IDEAS – SMOS Auxiliary Data File List	***1.66***
RD.20	SO-TN-UPC-PLM-0167	All LICEF mode implementation	***1.1*** *15/04/15*
RD.21	SO-IOP-ECE-TN-1368	Receiver and LFE Selection for ALL-LICEF Testing	***1.0*** *05/05/15*
RD.22	SO-TN-UPC-PLM-0161	IVT relative phase for Full-Pol mode	***1.0*** *23/10/13*
RD.23	SO-IOP-ECE-TN-1370	Heater Correction with Double Exponential	***0.2*** *05/07/16*
RD.24	-	BEC Presentation at SPCM28	*12/01/17*
RD.25	NIR-TN-HARP-029	Thermal Latency Correction Algorithm Theoretical Baseline Description	***1.1*** *28/09/17*

Ref.	Code	Title	Issue
RD.26	UPC Presentation at SPCM31	Improvements in Calibration	***1.0*** *27/09/17*
RD.27	CESBIO Presentation at SPCM31	The new AUX PATT	***1.0*** *13/12/17*

2. OVERVIEW

The document is organized as follows:

- Section 3 presents the generation method and origin of data for each of the Auxiliary Data Files
- Section 4 presents a description of the Auxiliary Data Files used by the processor.
- Section 5 lists the contents of the ADF Set 7.2.0
- Section 6 list the files in ADF Set 7.2.0

3. ADF GENERATION PROCEDURES

In this section, we will describe the procedures needed to generate the ADF files used during processing. Either by a full algorithmic description, when the algorithm is implemented in the L1OP, or by a description on how the files were generated externally.

3.1. AUX_GMAT

3.1.1. System Response definition

The instrument's System Response Function is determined by the following equation:

$$V_j^q(u) = \iint_{\xi^2+\eta^2\le 1} \frac{F_{n,j_1}^{p_1q_1}(\xi)\,F_{n,j_2}^{p_2q_2*}(\xi)}{\sqrt{\Omega_{j_1}^{p_1}\Omega_{j_2}^{p_2}}}\,\frac{T_B^p(\xi)-T_{Rec}\delta_p}{\zeta(\xi,\eta)}\,\hat{r}_{kj}(-\Delta t)\,e^{-j2\pi f_0\Delta t}\,d\xi d\eta \qquad \textbf{Eq. 1}$$

Where the following parameters are presented:

- $F_{n,j}^{pq}(\xi)$ is the normalised antenna radiation pattern of receiver j in polarisation p (co-polar if $q=p$ and cross-polar otherwise), expressed in cosine domain coordinates;
- Ω_j^p is the antenna solid angle of receiver j in polarisation p;
- T_{Rec} is the averaged physical temperature of the receivers, multiplied by the Dirac delta δ_p to represent that it is not applicable when the polarisation indexes p_1 and p_2 are not equal (i.e. full-polarisation);
- $\zeta(\xi,\eta) \equiv \sqrt{1-\xi^2-\eta^2}$ is the *Obliquity Factor*;
- $\hat{\hat{r}}_{kj}$ is the Fringe Washing Function term, normalised at the origin, that accounts for decorrelation effects in the path of the correlated signals;
- $\Delta t \equiv u\xi + v\eta + w\zeta(\xi,\eta)$ is the *Delay Time*;
- $d\xi d\eta$ represents the area of each (ξ,η) spatial sample in the integration domain.

For the rest of the document, wherever these equations are used, the off-plane component entering the Fringe Wash function and the exponential has been simplified to keep each equation in a single line (OF is the Obliquity Factor).

This equation relates the visibilities measured by the instrument, with the Brightness Temperature scene that is being observed. Due to the nature of the double integral, and expressing the visibilities and Brightness Temperatures matrices as vectors, this relationship can be expressed as a matrix-vector multiplication, hereafter referring this matrix as *G*-matrix.

$$V(u) = G(u;x_i)\left(T(x_i) - T_{rec}\right) \qquad \textbf{Eq. 2}$$

This G-matrix is dependent on the antenna patterns, the fringe washing function, the (u,v) frequency samples of V (w is the out of plane coordinate) and the spatial samples (ξ,η) of BT. In order to obtain the Brightness Temperature distribution that generated a certain measured calibrated visibilities, it is only required to invert G by whatever method is more appropriate.

The first step is to specify the (u,v) frequency samples, and corresponding spatial samples (ξ,η) for the resolution selected, that match the instrument configuration. The (u,v) frequency samples are determined by the location of the receivers in the instrument, whereas the spatial samples are simply chosen based on the desired sampling. The preferred option is to work with a resolution of 196x196 spatial samples. If greater resolution is desired, an interpolation may be performed after the reconstruction.

The visibilities measurements are taken at specific frequency samples. Being (x_1,y_1) and (x_2,y_2) the XY plane coordinates, and z_1,z_2 the off-plane coordinates of two antennas generating the visibility sample V_{12}, the corresponding frequency sample can be computed as:

$$(u_{12}, v_{12}, w_{12}) = \left(\frac{x_2 - x_1}{\lambda_0}, \frac{y_2 - y_1}{\lambda_0}, \frac{z_2 - z_1}{\lambda_0}\right) \qquad \textbf{Eq. 3}$$

Where λ_0 is the wavelength value at the central frequency of operation ($\lambda_0 = \frac{c}{f_0}$), for a typical value of f_0 of 1413.5MHz.

Computation of the spatial coordinates is done in a hexagonal grid but put in a rectangular matrix, according to the following formulation for an array steering of 30º. The corresponding frequency coordinates are also shown. Steering 30º means that the instrument is oriented with one of its arms (arm B) oriented 30º with respect to the flight direction.

Their outputs are two matrices with the coordinates of all points in the spatial and frequency domains according to the resolution specified:

$$(u,v) = \left(\frac{d}{2}(k_1 + 2k_2), \frac{\sqrt{3}d}{2}k_1\right)$$
$$(\xi,\eta) = \left(\frac{1}{N_T d}k_1, \frac{1}{\sqrt{3}N_T d}(k_1 + 2k_2)\right) \qquad \textbf{Eq. 4}$$

Where N_T is the resolution required (typically 196), d is the distance between adjacent receivers in wavelengths (typically 0.875), and k_1 and k_2 are the indexes of the matrix from 0 to N_T-1. It must be noticed that the computation has to be performed according to the "hexagonal quadrant" where the indexes are, since the centre baseline is the first element of the matrix; this accounts to subtracting N_T from the indexes depending on the part of the hexagon being retrieved.

Initially the G^{-1}-matrix shall be defined as the mathematical operator required to transform the 2556 complex calibrated visibilities plus the zero frequency value measured through the NIR elements

(2556+3), into the 196x196 reconstructed Brightness Temperature values and is described in the next chapters.

This operator is the inverse of the complete system response, described by a unique *G*-matrix, which takes as input the data produced in all polarisations (H, V and HV). This unique *G*-matrix includes the effect of cross-polarisation antenna patterns into the reconstruction. This *G*-matrix format is the same for all reconstruction methods; the only difference between reconstruction approaches lies in the external elements used to construct it.

The complete *G*-matrix (V=GT) is built for the full polarisation processing case. The output data are three vectors of calibrated visibilities: V_H with 2346 complex elements (2556 - NIR_XX_XX_V) plus 3 real elements from the NIR or LICEF measurement, V_V with the same amount of values 2346 (2556 - NIR_XX_XX_H) complex + 3 real and V_{HV} with 3303 complex elements. For information on this last case of V_{HV}, please refer to the document [RD.2]. The total number of output real valued elements shall then be (2346*2+3)*2+3303*2=15996.

In order to understand the origin of these numbers, it must be clear that in H or V polarisation, the amount of signals correlated is always 72, but of these only 69 are in either H or V polarisation. The remaining 3 are signals being correlated by the LICEF-NIR receivers in the opposite polarisation, so only 69*68/2 complex correlations are measured, which is the source for 2346. In NIR mode, the NIR elements are also measuring the total power of the image, which is the source for the remaining 3 real elements. In ALL-LICEF mode, since L1OP v7.0.0, this total power, or Brightness Temperature, can also be measured by the LICEFS – this means that the Antenna Patterns for the Dual-Pol part of the G/J+ for ALL-LICEF mode must be the average of the LICEF receivers used to compute the TA (see selected LICEFs in [RD21]).

The required inputs are the Brightness Temperature values in all polarisations. T_H and T_V are real valued, whereas T_{HV} is complex valued. Assuming a default size of 196x196, the total number of output real valued elements is 196x196*4=153664. Of course, the size can be reduced to 128x128 or 64x64, although a bigger sampling grid means that more detail is introduced in the System Response Function by using a finer antenna pattern grid.

Thus, the unique *G*-matrix shall be composed by 15996 rows and 153664 columns with real valued elements. Using a real valued matrix is preferred as it reduces the size and ensures that the input in Brightness Temperatures for H and V can be used as real valued.

Rows in the *G*-matrix are generated from particularising the general equation for a pair of LICEF receivers (*k, j* indexes) and polarisation values of the antenna patterns and Brightness Temperature (*p, q* indexes).

The rows shall be ordered as follows:

- The first 2346*2+3 rows shall correspond to H polarisation calibrated visibilities (p and q are H).
- The next 2346*2+3 rows shall correspond to V polarisation calibrated visibilities (p and q are V).
- The final 3303*2 rows shall correspond to HV polarisation calibrated visibilities (p is H and q is V).

In more detail and based on the following picture:

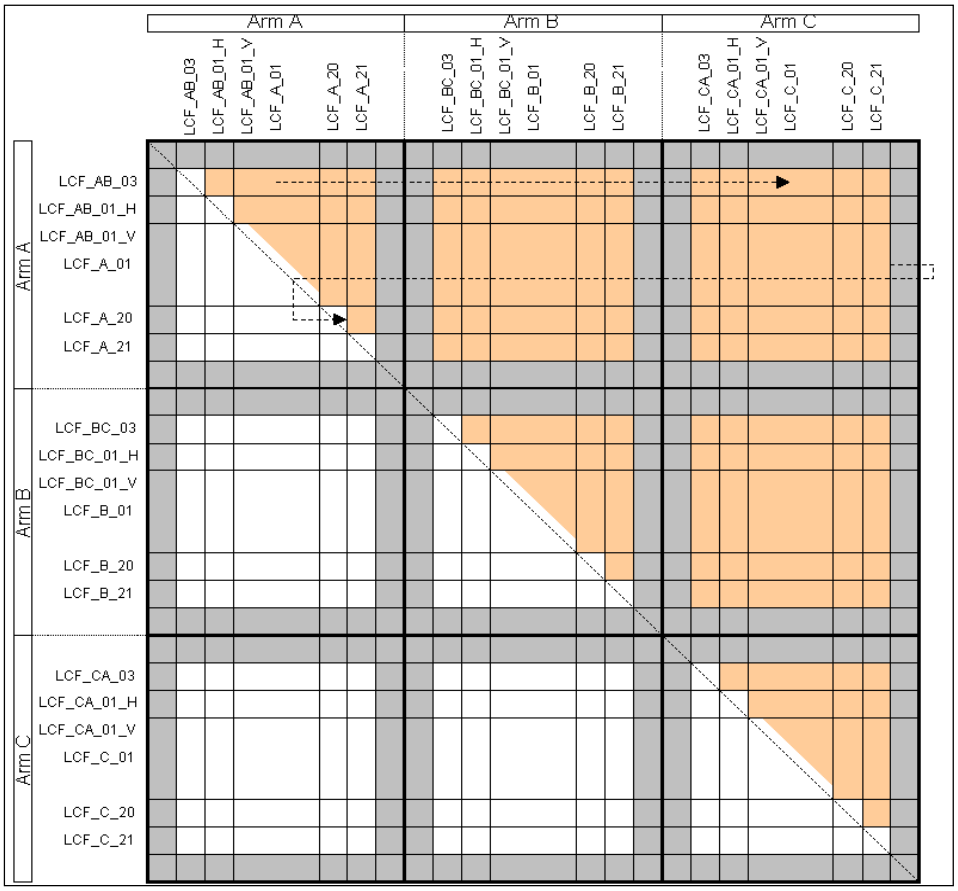

Figure 1: Calibrated Visibilities Matrix

- The first 3 rows shall correspond to the zero baselines as measured from the NIR or LICEFs for H polarisation. Depending on the ALL-LICEF configuration (OFF or ON), the order shall be first NIR_AB, then NIR_BC and last NIR_CA or the same average LICEF Antenna Pattern for the first 3 rows.
- The next 2346 rows shall correspond to the real values of the H polarisation calibrated visibilities as received from the L1a products, and ordered in the same approach as shown in figure 11 in chapter 4.3.1.3 of [AD.13]. i.e. first element shall be calibrated visibility of LICEF_AB_03 against LICEF_AB_01_H, next shall be LICEF_AB_03 against LICEF_A_01, etc… until the sixty ninth element LICEF_AB_03 against LICEF_C_21. The next element shall then be LICEF_AB_01_H against LICEF_A_01, and so on until LICEF_AB_01 against LICEF_C_21. The next shall be LICEF_A_01 against LICEF_A_02, etc. until LICEF_A_02 against LICEF_C_21. This ordering shall continue until all LICEF correlations have been inserted, and not including correlations with LICEF_NIR in V polarisation (i.e. correlations with receivers LICEF_AB_01_V, LICEF_BC_01_V and LICEF_CA_01_V)
- The next 2346 rows shall correspond to the imaginary values of the H polarisation calibrated visibilities, following the same order as above.

- The next 3 rows shall correspond to the zero baselines as measured from the NIR or LICEFs for V polarisation. Depending on the ALL-LICEF configuration (OFF or ON), the order shall be first NIR_AB, then NIR_BC and last NIR_CA or the same average LICEF Antenna Pattern for the first 3 rows.
- The next 2346 rows shall correspond to the real values of the V polarisation calibrated visibilities as received from the L1a products, and ordered in the same approach as shown in figure 11 of [AD.13]. i.e. first element shall be calibrated visibility of LICEF_AB_03 against LICEF_AB_01_V, next shall be LICEF_AB_03 against LICEF_A_01, etc… until the sixty ninth element LICEF_AB_03 against LICEF_C_21. The next element shall then be LICEF_AB_01_V against LICEF_A_01, and so on until LICEF_AB_01 against LICEF_C_21. The next shall be LICEF_A_01 against LICEF_A_02, etc. until LICEF_A_02 against LICEF_C_21. This ordering shall continue until all LICEF correlations have been inserted, and not including correlations with LICEF_NIR in H polarisation (i.e. correlations with receivers LICEF_AB_01_H, LICEF_BC_01_H and LICEF_CA_01_H).
- The next 2346 rows shall correspond to the imaginary values of the V polarisation calibrated visibilities, following the same order as above.
- The next 3303 rows shall correspond to the real values of the HV polarisation calibrated visibilities as received from the L1a products, and ordered according to the following approach. Please refer to figures 10 and 11 of [RD.2] (orange cells) for a visual representation of the description:
  - First 528 rows with calibrated visibilities of elements in Arm A in H polarisation against elements in Arm B in V polarisation. I.e. first LICEF_AB_03 against LICEF_BC_03, then LICEF_AB_03 against LICEF_BC_01_V, then LICEF_AB_03 against LICEF_B_01, until the 23rd element LICEF_AB_03 against LICEF_B_21. Next is LICEF_AB_01_H against LICEF_BC_03, then LICEF_AB_01_H against LICEF_B_01, and so on until all elements in arm B are correlated with LICEF_AB_01_H (Please note that this row does not include the correlation against LICEF_BC_01_V). This ordering continues until the last element correlated is LICEF_A_21 against LICEF_B_21.
  - Next 528 rows with calibrated visibilities of elements in arm A in H polarisation against elements in arm C in V polarisation. Same order as above, i.e. first LICEF_AB_03 against LICEF_CA_03, then LICEF_AB_03 against LICEF_CA_01_V, then LICEF_AB_03 against LICEF_C_01, until the 23rd element LICEF_AB_03 against LICEF_C_21. Next is LICEF_AB_01_H against LICEF_CA_03, then LICEF_AB_01_H against LICEF_C_01, and so on until all elements in arm C are correlated with LICEF_AB_01_H (Please note that this row does not include the correlation against LICEF_CA_01_V). This ordering continues until the last element correlated is LICEF_A_21 against LICEF_C_21.
  - Next 528 rows with calibrated visibilities of elements in arm B in H polarisation against elements in arm A in V polarisation. Same order as above, i.e. first LICEF_BC_03 against LICEF_AB_03, then LICEF_BC_03 against LICEF_AB_01_V, then LICEF_BC_03 against LICEF_A_01, until the 23rd element LICEF_BC_03 against LICEF_A_21. Next is LICEF_BC_01_H against LICEF_AB_03, then LICEF_BC_01_H against LICEF_A_01, and so on until all elements in arm A are correlated with LICEF_BC_01_H (Please note that this row does not include the correlation against LICEF_AB_01_V). This ordering continues until the last element correlated is LICEF_B_21 against LICEF_A_21.

- Next 528 rows with calibrated visibilities of elements in arm B in H polarisation against elements in arm C in V polarisation. Same order as above, i.e. first LICEF_BC_03 against LICEF_CA_03, then LICEF_BC_03 against LICEF_CA_01_V, then LICEF_BC_03 against LICEF_C_01, until the 23rd element LICEF_BC_03 against LICEF_C_21. Next is LICEF_BC_01_H against LICEF_CA_03, then LICEF_BC_01_H against LICEF_C_01, and so on until all elements in arm C are correlated with LICEF_BC_01_H (Please note that this row does not include the correlation against LICEF_CA_01_V). This ordering continues until the last element correlated is LICEF_B_21 against LICEF_C_21.
- Next 528 rows with calibrated visibilities of elements in arm C in H polarisation against elements in arm A in V polarisation. Same order as above, i.e. first LICEF_CA_03 against LICEF_AB_03, then LICEF_CA_03 against LICEF_AB_01_V, then LICEF_CA_03 against LICEF_A_01, until the 23rd element LICEF_CA_03 against LICEF_A_21. Next is LICEF_CA_01_H against LICEF_AB_03, then LICEF_CA_01_H against LICEF_A_01, and so on until all elements in arm A are correlated with LICEF_CA_01_H (Please note that this row does not include the correlation against LICEF_AB_01_V). This ordering continues until the last element correlated is LICEF_C_21 against LICEF_A_21.
- Next 528 rows with calibrated visibilities of elements in Arm C in H polarisation against elements in Arm B in V polarisation. Same order as above, i.e. first LICEF_CA_03 against LICEF_BC_03, then LICEF_CA_03 against LICEF_BC_01_V, then LICEF_CA_03 against LICEF_B_01, until the 23rd element LICEF_CA_03 against LICEF_B_21. Next is LICEF_CA_01_H against LICEF_BC_03, then LICEF_CA_01_H against LICEF_B_01, and so on until all elements in arm B are correlated with LICEF_CA_01_H (Please note that this row does not include the correlation against LICEF_BC_01_V). This ordering continues until the last element correlated is LICEF_C_21 against LICEF_B_21.
- Next 23 rows with calibrated visibilities of LICEF_AB_01_H against all other receivers in arm A in V polarisation. I.e. LICEF_AB_01_H against LICEF_AB_03, LICEF_AB_01_H against LICEF_AB_01_V, LICEF_AB_01_H against LICEF_A_01, etc… until LICEF_AB_01_H against LICEF_A_21
- Next 22 rows with calibrated visibilities of all receivers in arm A in H polarisation against LICEF_AB_01_V, excluding LICEF_AB_01_H against LICEF_AB_01_V, whose equation is presented in the point above. I.e. LICEF_AB_03 against LICEF_AB_01_V, LICEF_A_01 against LICEF_AB_01_V, etc… until LICEF_A_21 against LICEF_AB_01_V
- Next 23 rows with calibrated visibilities of LICEF_BC_01_H against all other receivers in arm B in V polarisation. I.e. LICEF_BC_01_H against LICEF_BC_03, LICEF_BC_01_H against LICEF_BC_01_V, LICEF_BC_01_H against LICEF_B_01, etc… until LICEF_BC_01_H against LICEF_B_21
- Next 22 rows with calibrated visibilities of all receivers in arm B in H polarisation against LICEF_BC_01_V, excluding LICEF_BC_01_H against LICEF_BC_01_V, whose equation is presented in the point above. I.e. LICEF_BC_03 against LICEF_BC_01_V, LICEF_B_01 against LICEF_BC_01_V, etc… until LICEF_B_21 against LICEF_BC_01_V
- Next 23 rows with calibrated visibilities of LICEF_CA_01_H against all other receivers in arm C in V polarisation. I.e. LICEF_CA_01_H against LICEF_CA_03, LICEF_CA_01_H against LICEF_CA_01_V, LICEF_CA_01_H against LICEF_C_01, etc… until LICEF_CA_01_H against LICEF_C_21

- Next 22 rows with calibrated visibilities of all receivers in arm C in H polarisation against LICEF_CA_01_V, excluding LICEF_CA_01_H against LICEF_CA_01_V, whose equation is presented in the point above. I.e. LICEF_CA_03 against LICEF_CA_01_V, LICEF_C_01 against LICEF_CA_01_V, etc… until LICEF_C_21 against LICEF_CA_01_V

- The following and last 3303 rows shall correspond to the imaginary values of the HV polarisation calibrated visibilities as received from the L1a products, and ordered in the approach that has been just described.

Columns in the *G*-matrix are generated from particularising the general equation for a certain pair of coordinates in the antenna frame (ξ-η indexes) and polarisation values of the antenna patterns and Brightness Temperature (*p, q* indexes).

The order of the columns shall be the following:

- The first 196x196 columns shall correspond to H polarisation Brightness Temperatures
- The next 196x196 columns shall correspond to V polarisation Brightness Temperatures
- The next 196x196 columns shall correspond to the real components of the HV polarisation Brightness Temperatures
- The final 196x196columns shall correspond to the imaginary components of the HV polarisation Brightness Temperatures

Going into more detail, each distribution of 196x196 elements shall correspond to the SMOS natural hexagonal grid represented in a rectangular matrix. The centre (0,0) shall be the first element of the distribution. As an example, the following figures show the resulting ξ-η distribution of values for a 128x128 Brightness Temperature scene using steering 30º of MIRAS instrument:

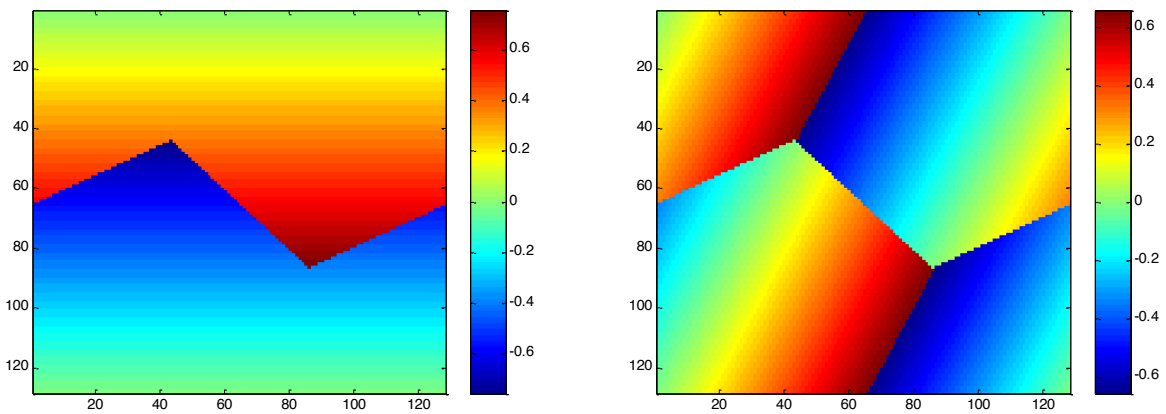

Figure 2: ξ (left image) and η (right image) coordinates proposed for the G-matrix format

The ordering of the antenna patterns should follow the one shown in the following image:

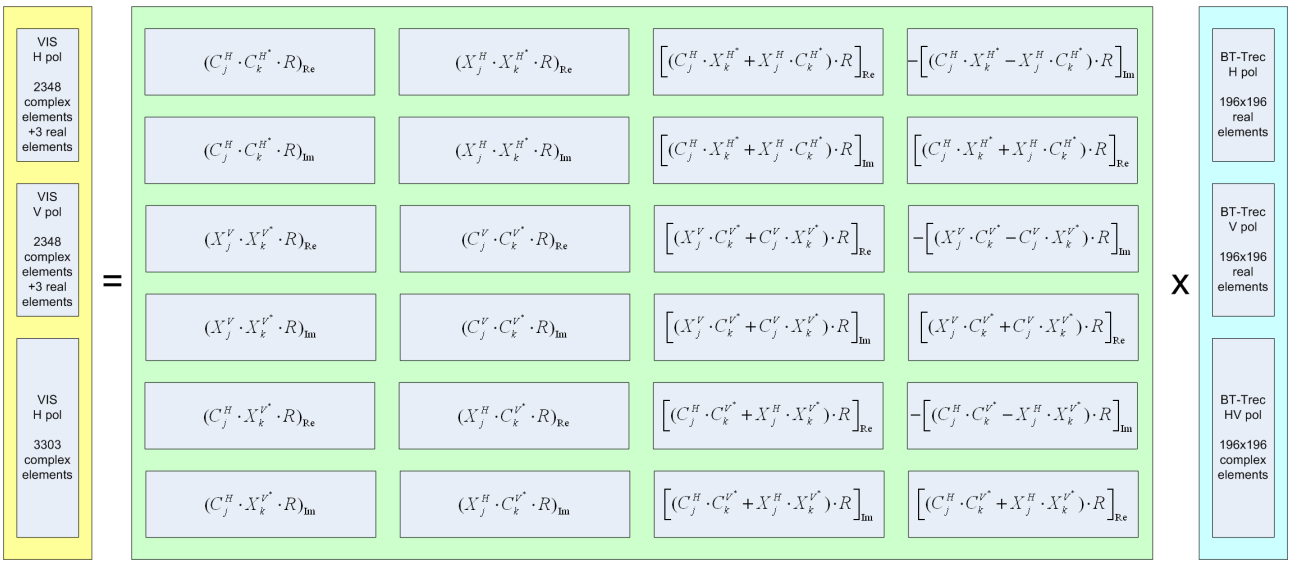

Figure 3: G-matrix Decomposition. C and X are co- and cross-polar Antenna Patterns and R is the Fringe Wash Function multiplied by the complex exponential term (see Eq. 5)

If the level of the cross-polarisation patterns is negligible when compared to the co-polar patterns (to be addressed in a foreseen study), then the above *G*-matrix may be split into three independent *G*-matrices, each one related to one polarisation only. The format of the H and V polarisation *G*-matrix shall be the same, while the HV *G*-matrix shall be a bit bigger as shown above.

The fringe washing function will be calibrated in orbit for several baselines (those sharing noise sources), and it shall be estimated for the rest of baselines. Again, depending on the image reconstruction method, the FWF calibration shall be applied differently.

3.1.2. On-ground characterised G-matrix

This *G*-matrix is built based solely on input data available, such as calibration data and auxiliary data files. In order to calculate the *G*-matrix the following equation is used:

$$G(\mathbf{u};\mathbf{x}) = \frac{\hat{F}_k(\boldsymbol{\xi})\hat{F}_j^*(\boldsymbol{\xi})}{\zeta(\boldsymbol{\xi})\sqrt{\Omega_{j_1}\Omega_{j_2}}}\hat{\tilde{r}}_{kj}(-\Delta t)e^{-j2\pi f_0 \Delta t}d\boldsymbol{\xi} \qquad \textbf{Eq. 5}$$

As we can see using this equation it is possible to calculate all the matrix elements using the Fringe Wash Function , $\hat{\tilde{r}}$, Antenna Patterns, $\hat{F}$, the solid angle of the antennas, Ω, and the spatial and frequency coordinates ($\boldsymbol{u}, \boldsymbol{\xi}$).

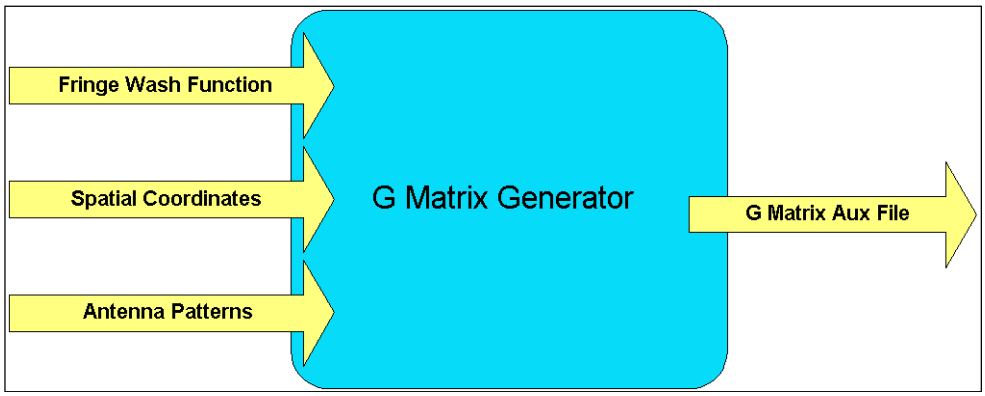

Figure 4: G-matrix Processor

3.1.2.1. Antenna Patterns

Antenna patterns were measured once on the ground, and a static Auxiliary Data File was generated with the measurements in the spherical coordinates (ɵ,ϕ) using a grid 181x141. The antenna patterns are also measured at three different frequencies: the central operation frequency and another two at plus and minus a B bandwidth.

The file used in L1OP is generated by applying several pre-processing steps. First, replace in X polarization LICEF A05 by the average of its neighbours, A04 and A06, and multiply the 69 cross-polar patterns by -1. The patterns of the three frequencies in the complex plane are then averaged, interpolated to the 196x196 hexagonal grid covering the whole unit circle (see Figure 5) and normalized by the solid angles computed using equation (1) in [RD.4].

Finally, the Antenna Patterns for the hinges outside the hub are replaced by their neighbours [RD.3] as described in Table 3-1. Table 3-1: Elements with Antenna Patterns to be replaced

Original Hinge	*Hinge to use as replacement*
A_09	A_08
A_10	A_11
A_15	A_14
A_16	A_17
B_09	B_08
B_10	B_11
B_15	B_14
B_16	B_17
C_09	C_08
C_10	C_11

C_15	C_14
C_16	C_17

The full processing was described in [RD.27].

3.1.2.2. Fringe Wash Function

The Fringe Washing Function shape shall be calibrated/estimated as part of the nominal calibration campaign, by injecting correlated noise and introducing time lags in the correlated signals. An L1a product file shall be generated every time this type of calibration is performed.

$$\hat{\tilde{r}}_{\mathrm{j}}(\tau) \approx A \cdot \mathrm{sinc}\left(B \cdot (\tau - C)\right) \cdot e^{i\left(D\tau^2 + E\tau + F\right)} \qquad \textbf{Eq. 6}$$

The way to compute the different coefficients is shown in [AD.11]. The equations to be used are:

$$\begin{aligned} \left|g_{\mathrm{j}}(-T_S)\right| &\approx A \cdot \mathrm{sinc}\left(B \cdot (-T_S - C)\right) \\ \left|g_{\mathrm{j}}(0)\right| &\approx A \cdot \mathrm{sinc}\left(B \cdot C\right) \\ \left|g_{\mathrm{j}}(+T_S)\right| &\approx A \cdot \mathrm{sinc}\left(B \cdot (T_S - C)\right) \end{aligned} \qquad \textbf{Eq. 7}$$

$$\begin{aligned} D^{H,V} &= \left(\frac{\arg\left(g_{\mathrm{j}}^{H,V}(+T_S)\right) + \arg\left(g_{\mathrm{j}}^{H,V}(-T_S)\right)}{2} - \arg\left(g_{\mathrm{j}}^{H,V}(0)\right) \right) \frac{1}{T_S^2} \\ E^{H,V} &= \frac{\arg\left(g_{\mathrm{j}}^{H,V}(+T_S)\right) - \arg\left(g_{\mathrm{j}}^{H,V}(-T_S)\right)}{2} \frac{1}{T_S} \\ F^{H,V} &= \arg\left(g_{\mathrm{j}}^{H,V}(0)\right) \end{aligned} \qquad \textbf{Eq. 8}$$

The FWF is measured independently for the paths of the in-phase and quadrature signals, meaning that for the same visibility, there shall be two different values of the FWF. One is applicable to the real part component of the visibility, while the other is applicable to the imaginary part of the component. The following equation shows this behaviour in detail:

$$\begin{matrix}\mathrm{Re}\\ \mathrm{Im}\end{matrix}\left\{G_{\mathrm{j}}(\xi)\right\} = \begin{matrix}\mathrm{Re}\\ \mathrm{Im}\end{matrix}\left\{ \frac{\hat{F}_{j_1}^{p_1 q_1}(\xi)\hat{F}_{j_2}^{p_2 q_2^*}(\xi)}{\zeta(\xi)\sqrt{\Omega_k \Omega_j}} \begin{Bmatrix} \hat{r}_{i_k i_j}(-\Delta t_{\mathrm{j}}) \\ \hat{r}_{q_k i_j}(-\Delta t_{\mathrm{j}}) \end{Bmatrix} e^{-j2\pi f_0 \Delta t_{\mathrm{j}}} d\xi \right\} \qquad \textbf{Eq. 9}$$

It has to be remarked that the FWF shape is used in the *G*-matrix computation is normalised with the FWF at the origin. This means for example that the final application of the A and F coefficients will change slightly from what has been explained in the previous equations.

3.1.2.3. LICEF Spatial Coordinates

The LICEF coordinates are used to compute the applicable (*u,v*) baselines as per Eq. 4 can be taken from their initial measured positions in an Auxiliary Data File, or an elastic model may be applied to obtain them as a function of time. Regardless of the approach, UPC has already modelled deviations or errors in the receivers' positions as an error in the retrieved Brightness Temperatures.

3.1.3. Expanded Hexagonal Domain in the G-matrix

In the current definition of the Hexagonal G-Matrix, the Unit-Circle is circumscribed by a hexagon, i.e., with $N_T = 196$. This (ξ, η) grid is represented in Figure 5 with the green circles, along with the other grids used in L1OP.

The impact of this modification of the grid resolution is that the size of the G-matrix changes from 4x128x128 (65536) to 4x196x196 (153664) columns, yielding an increase of the G-matrix size from ~8 GiB to ~20GiB.

All the other steps in the computation of the G-matrix are the same as described previously.

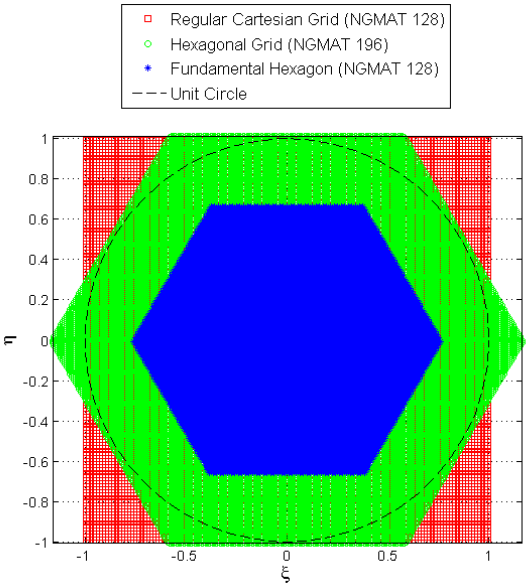

Figure 5: (ξ, η) Grids used in L1OP

3.1.4. ALL-LICEF G-Matrix

Since L1OP v700, the ALL-LICEF mode was implemented. In this mode the Antenna Temperature is no longer measured by the NIRs but it is computed by a weighted average of the LICEF Antenna Temperatures ([RD.20] and [RD.21]).

To account for this, the Antenna Patterns in the first three rows have to be computed as the average of the Antenna Patterns of selected LICEFs – but only for the Dual Pol section of the G-matrix. For that reason, the first three rows of the Dual Pol section will be identical. The HV section remains unchanged and the NIR cross-polar patters are still used.

3.1.5. System Response Function Mathematical Inversion

The mathematical inversion of the *G*-matrix is based on a band-limited regularisation, which is equivalent to:

$$\begin{cases} \min_{T \in \hat{\ }} \left\| V - GT \right\|^2 \\ (I - P_H)T = 0 \end{cases} \qquad \textbf{Eq. 10}$$

where P_H plays the role of a regularisation parameter.

This method consists in a reduction of the domain applicability, by creating the *J* -matrix. The *G*-matrix operates between Calibrated Visibilities and Brightness Temperatures, whereas the J Matrix operates between Calibrated Visibilities and Brightness Temperature Frequencies $\hat{T}$.

Secondly, the *J*-matrix is mathematically inverted using a minimum norm approach, so that the Brightness Temperature Frequencies may be obtained after a simple matrix-vector multiplication ($J^{I}*V$)

3.1.6. Implementation

As it was described before, the *G*-matrix is used in two processing units, in the *G*-matrix multiplication unit, to generate the Delta Visibilities from the calculated temperatures, and for the *J*-matrix generation.

To generate the *G*-matrix, the L1 processor follows the processing steps described in the next diagram.

The first step is to compute the spatial coordinates, where the result will be the 196x196 (ξ,η) coordinates. The default option is to use the expanded hexagonal G-matrix (HEXAGON_UNIT_CIRCLE), which is defined in an hexagonal grid defined with Eq. 4 and with $N_T = 196$.

After the (ξ,η) coordinates calculations, the antenna patterns coming from the pre-processing applied in Section 3.1.2.1 are used in Eq. 5. The following step is the computation of the Fringe Wash Function shape according to the Eqs. 6, 7 and 8.

Finally, after all the previous steps we apply the Eq. 5 to generate the on-ground characterised *G*-matrix and to produce an Auxiliary Data File for the Delta Visibilities *G*-matrix or a temporary file for the *J*-matrix generation. For each pair of receivers, the LICEF coordinates are loaded into memory and *u*, *v* and *w* are calculated using Eq. 3.

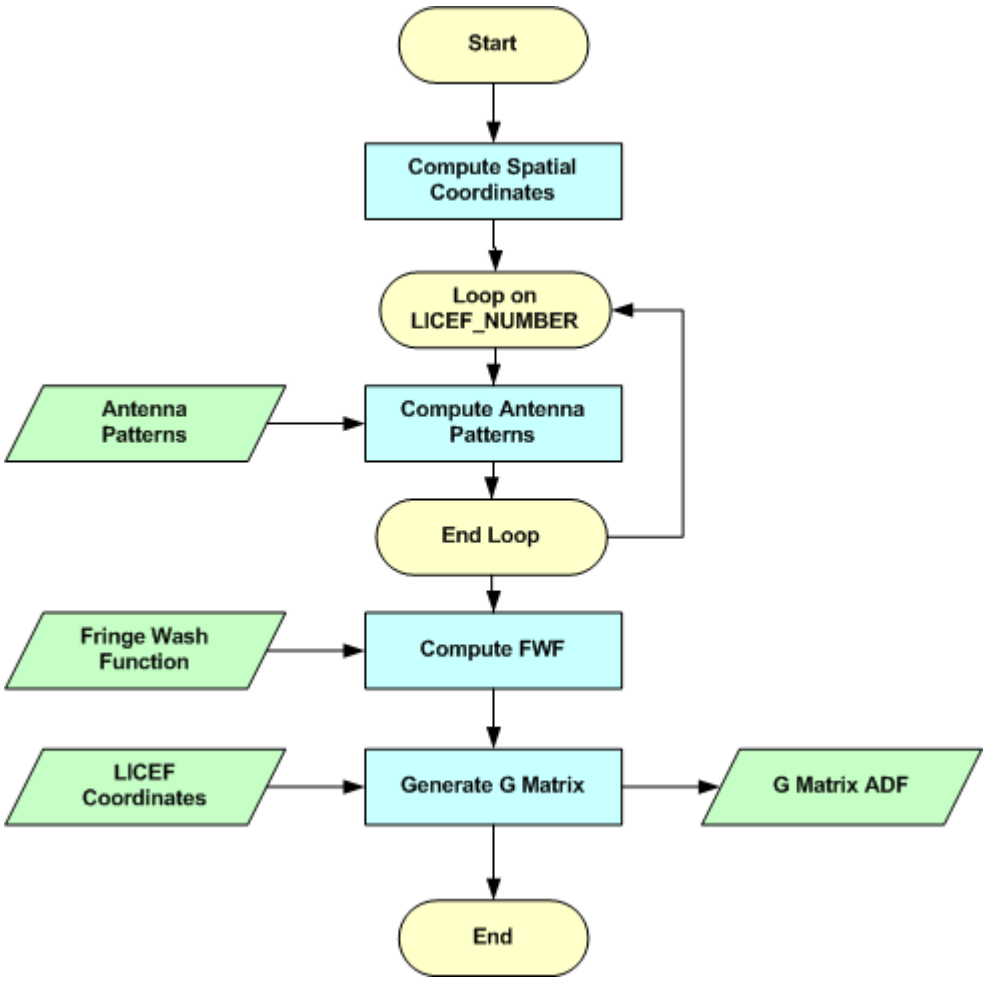

Figure 6: On-ground characterised G-matrix Generation

3.1.6.1. Inputs

- Auxiliary file with antenna amplitude and phase patterns (SM_xxxx_AUX_PATT##_<ID>).
- Auxiliary file with Weights per frequency and Normalization factors per LICEF (SM_xxxx_AUX_PLM__<ID>).
- Auxiliary file with LICEF positions (SM_xxxx_AUX_PLM__<ID>).
- L1a Fringe Wash Function File with the estimated coefficients used in the computation of the *G*-matrix (SM_xxxx_MIR_FWAS1A<ID>).

3.1.6.2. Outputs

- *G*-matrix auxiliary file to be used in the Foreign Sources Correction and Image Reconstruction Process (SM_xxxx_AUX_GMAT__<ID>).

3.1.6.3. List of Variables

The following table describes the variables used in the subsequent implementation section. Variables are listed as input, local and output (I, L, O). The *Size* column indicates the number of elements constituting that variable, and NOT the size of the variable in bytes (this information can be taken from the *Type* column).

Variable name	Description	Definition	Type	Class	Unit	Size
fwf_filename	Fringe Wash Function ADF.	N/A	char	I	N/A	Pointer
antenna_patterns_filename	Antenna Patterns ADF filename	N/A	char	I	N/A	Pointer
ap_correction_factors	Weights to apply to each Frequency and Normalization factors	N/A		I	N/A	Pointer
antenna_patterns	Antenna Patterns	N/A		L		
fwf_corrected	Fringe Wash function computed	Eq. 8		L	N/A	
spatial_coordinates	Spatial coordinates computed	Eq. 4		L		
gmatrix	*G*-matrix data.	Eq. 5	double	O	N/A	[15996] x [4*196*196]

Table 3-2: On-ground characterised G-matrix Variable List

3.1.6.4. Implementation details

The function ***generate_gmatrix*** is presented below. It represents a first approach with the methods needed to generate the on-ground characterised *G*-matrix.

First the (ξ,η) coordinates matrices are generated. These matrices are different depending on the *G*-matrix type. If it is the "HEXAGON" the function ***computeCoordinates*** will be the following:

```
for i=0:N-1
for j=0:N-1
   if ((i+j) > N)
       ii = i-N; jj = j-N;
       if ((i-2*j)   >  0)  ii = i-N; jj = j;   end
       if ((2*i-j)   <= 0)  ii = i;   jj = j-N; end
   else
       ii = i;   jj = j;
       if ((2*i-j-N) >  0)  ii = i-N; jj = j;   end
       if ((i-2*j+N) <= 0)  ii = i;   jj = j-N; end
   end
   X(i+1,j+1) = (0.5*sqrt(3)*jj)*dx;
   Y(i+1,j+1) = (ii - 0.5*jj)*dx;
end
end
The same for (u,v) grid:
for i=0:N-1
for j=0:N-1
   if (i > j)
       ii = i-N; jj = j;
       if ((2*i+j-N)   <  0)  ii = i;   jj = j;   end
       if ((i+2*j-2*N) >  0)  ii = i-N; jj = j-N; end
   else
       ii = i; jj = j-N;
       if ((i+2*j-N)   <= 0)  ii = i;   jj = j;   end
       if ((2*i+j-2*N) >= 0)  ii = i-N; jj = j-N; end
   end
   U(i+1,j+1) = (jj + 0.5*ii)*du;
   V(i+1,j+1) = (0.5*sqrt(3)*ii)*du;
end
end
```

with $N = 196$.

In the case of the “UNIT_CIRCLE” *G*-matrix the ***computeCoordinates*** function will have the following source code:

```
step = 2.0 / (N_GMAT);
for (i = 0; i < N; i++){
    for (j = 0; j < N_GMAT; j++){
        xi[i][j] = (-1 + (step/2))  + (i*step);
        eta[i][j] = (-1 + (step/2))  + (j*step);
    }
}
```

```
#define N 196
error = computeCoordinates(xi, eta);
error = computeAntennaPatterns(antenna_patterns_filename, xi, eta,
antenna_patt_corrected);
error = computeFWFshape(fwf_filename, u, v, xi, eta, fwf_coefs);
for(i=0; i!=LICEF_NUMBER; ++i){
  for(j=0; j!=LICEF_NUMBER; ++j){
   error = computeReceiverPositions(licef_coordinates_data, i, j, &u, &v, &w);
   for(int k=0; k!=N; ++k){
      for(int l=0; l!=N;++l){
             switch(pol_mod){
              case H, V or HV:
                    error = prepareFWF(pol_mode, i, j, k, l, fwf_shape, fwf_coefs);
                    g_element = (1/(sqrt(1-(xi*xi)(eta*eta))))*(antenna_patt_corrected)*
             (fwf_coefs)*exp(sqrt(-1)*2*PI*(u*xi+v*eta);
                    error = addGelement(g_element);
           break;
      }
    }
  }
}
```

The *G*-matrix is computed based on Eq. 5, but first the antenna patterns and the fringe wash function shape must be obtained. The LICEF coordinates must also be loaded in memory.

compute_fwf_shape method applies Eq. 6 to get the fringe wash function shape ready to compute the *G*-matrix. This function will return the A, B, C, D, E, and F Fringe Wash Function coefficients needed to compute each value of the *G*-matrix, depending on polarization mode. The method receives an averaged Fringe Wash Function product and extracts the coefficients A, B, C, D and E. F is not needed, and can be set to zero, as the FWF shape used in the *G*-matrix generation is normalised.

The phase coefficients D, E and F are obtained immediately for each baseline by simply applying Eq. 8. The magnitude coefficients must be computed using a Newton-Raphson method by approximating the values in Eq. 7 to a sinc function. The implementation is shown below for each baseline *k*:

```
/* FWF values at +T and -T must be normalized to the origin*/
fwf1_abs = fwf1_abs / fwf0_abs; //FWF at -T
fwf2_abs = fwf2_abs / fwf0_abs; //FWF at +T
/*initial solution for Newton Raphson*/
counter = 0; error = 100; //timestep is the value of +T
p1 = (fwf2_abs - fwf1_abs) * timestep / (fwf2_abs + fwf1_abs -2.);
p2 = -2. * timestep * timestep / (fwf2_abs + fwf1_abs -2.);
AII[k] = 1. + p1 * p1 / 4. / p2;
BII[k] = sqrt(6. / AII[k] / p2) / PI;
CII[k] = -p1 / 2.;
/*avoid singularities when fwf2_phase = fwf1_phase*/
if (fabs(fwf2_abs - fwf1_abs) > eps)
{
   solution[0] = PI * BII[k] * timestep;
   solution[1] = PI * BII[k] * CII[k];
   while (fabs(error) > eps && counter < 100)
   {
      vector[0] = (fwf1_abs * (solution[0] + solution[1]) * sin(solution[1])) - solution[1]
* sin(solution[0] + solution[1]);
      vector[1] = (fwf2_abs * (-solution[0] + solution[1]) * sin(solution[1])) -
solution[1] * sin(-solution[0] + solution[1]);
      jacobian[0] = fwf1_abs * sin(solution[1]) - solution[1] * cos(solution[0] +
solution[1]);
      jacobian[2] = fwf1_abs * sin(solution[1]) + fwf1_abs * (solution[0] + solution[1]) *
cos(solution[1]) - (sin(solution[0] + solution[1]) + solution[1] * cos(solution[0] +
solution[1]));
      jacobian[1] = -fwf2_abs * sin(solution[1]) + solution[1] * cos(-solution[0] +
solution[1]);
      jacobian[3] = fwf2_abs * sin(solution[1]) + fwf2_abs * (-solution[0] + solution[1]) *
cos(solution[1]) - (sin(-solution[0] + solution[1]) + solution[1] * cos(-solution[0] +
solution[1]));
      dgesv_(&n, &nrhs, jacobian, &n, ipiv, vector, &n, &info);
      solution[0] -= vector[0];
      solution[1] -= vector[1];
      error = vector[0]*vector[0] + vector[1]*vector[1];
      counter++;
   }
   BII[k] = solution[0] / timestep / PI;
   AII[k] = 1. / sinc(-solution[1] / PI);
```

In the specific case that the magnitude of FWF at +T and –T are exactly equal, the above resolution cannot be performed, so another approximation must be implemented.

```
else /*singular case where fwf2_abs = fwf1_abs, cannot use Newton Raphson*/
{
   solution[0] = PI * BII[k] * timestep;
   while (fabs(error) > eps && counter < 100)
   {
      vector[0] = fwf1_abs * solution[0] - sin(solution[0]);
      jacobian[0] = fwf1_abs - cos(solution[0]);
      solution[0] -= (vector[0]/jacobian[0]);
      error = vector[0]/jacobian[0];
      counter++;
   }
   BII[k] = solution[0] / timestep / PI;
   AII[k] = 1.;
   CII[k] = 0.;
}
```

With this code, the FWF shape amplitude coefficients are computed normalised to the FWF value at the origin.

For each pair of LICEFs the receiver positions must be calculated using Eq. 3, which returns the values of the ($\underline{u,v,w}$)-coordinates generating the visibility sample $V_{\mathbf{j}}$.

The G-matrix element is calculated using Eq. 9 where the real part uses the fringe wash function shape ii ($\hat{\hat{r}}_{i_k i_j}$) and the imaginary part uses the function shape qi ($\hat{\hat{r}}_{q_k i_j}$).At this point the two antenna patterns that build up the (k, j) baseline being processed are averaged according to the weights specified and renormalized with the correction factors provided in [RD.4].

The method ***add_g_element*** will add the elements to the G-matrix and each value will be stored as double. The real part for each polarization mode is stored in the first 2346 lines and the imaginary in the next 2346. With this approach the future operations are easier to implement since the real part is already separated form the imaginary part. In the HV part there will be two columns, one with the real part and other with the imaginary and instead of 2346 lines there will be 3303.

The row order used in the G-matrix generation is described in a previous section of the document (Section 3.1).

The resulting G-matrix must be order by 4x196x196 columns (corresponding to the (ξ,η) coordinates) and 15996 lines (corresponding to the pairs of LICEFs).

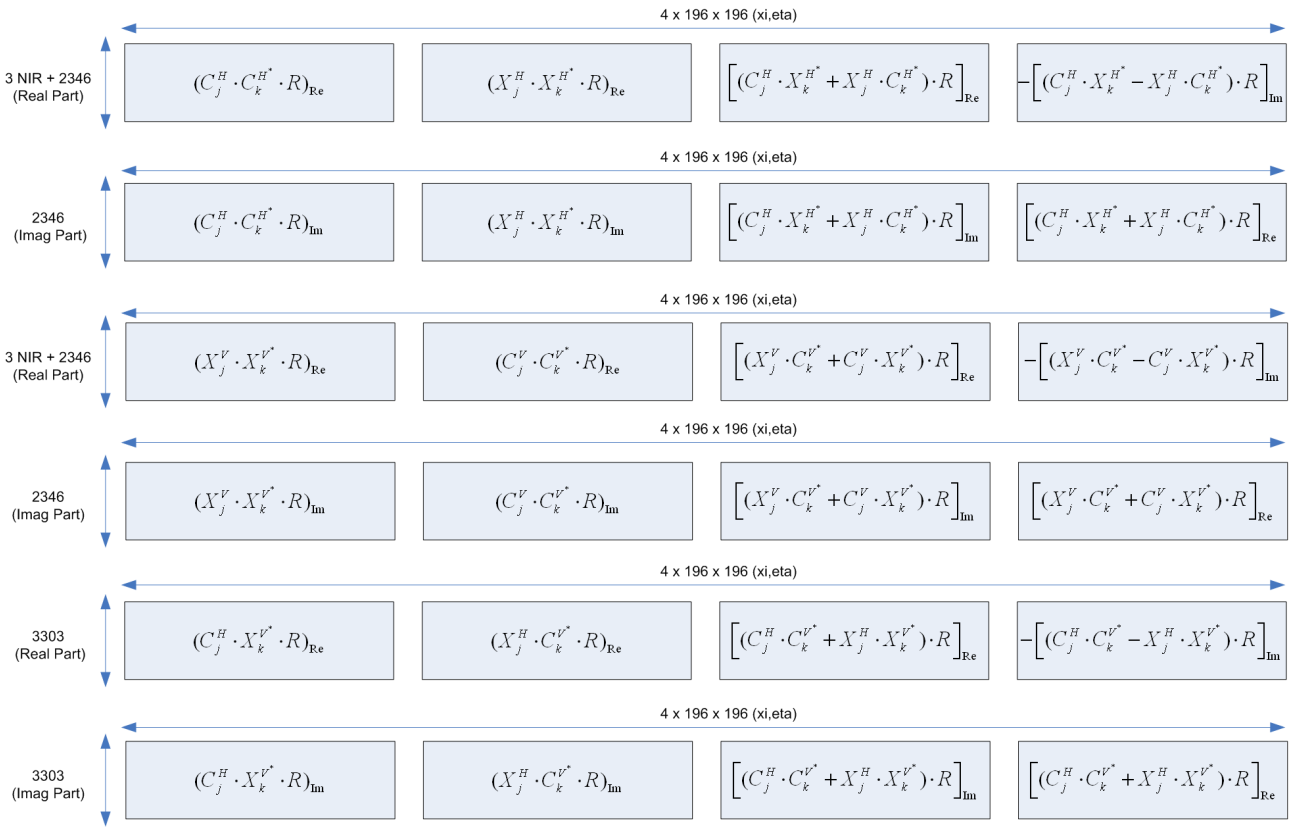

Figure 7: G-matrix Order (see Figure 3***)***

In the previous figure it is demonstrated how the *G*-matrix lines and columns are ordered.

For the zero-baseline the Fringe Wash Function shape is not needed. The real part of Fringe Wash is 1 and the imaginary 0, since there is no correlation between receivers.

It is very important to store in the *G*-matrix header the correlator layer (Nominal or Redundant) that was active when the FWF shape was measured. This value can be retrieved from the FWF shape product header, and it is required in order to determine which data can be reconstructed with the *G*-matrix product.

3.2. AUX_JMAT

This matrix represents the mathematical reduction of the previous *G*-matrix in order to obtain Brightness Temperatures frequencies. It represents the System Response Function of the instrument transforming Calibrated Visibilities plus the zero frequency value measured through the NIR elements into Brightness Temperature Frequencies.

This is the matrix that shall be inverted to complete the Image Reconstruction process. Regardless of how the *G*-matrix is built, the size of the Brightness Temperature grid, or what modelling it has used, its reduction into the *J*-matrix shall always have the same format and size.

The number of columns is now dependent on the (*u,v*) frequency domain, and is restricted to the number of non-redundant correlations that the instrument shall be measuring. For MIRAS, the number of non-redundant visibilities is 2791, forming a star shape in the (*u,v*) plane, and is only dependent on the number of receivers per arm and the Y shape of the instrument.

Thus, the number of columns for this matrix shall be 11164. This number comes from 1395 complex elements plus one real element that is measured for H or V polarisation, plus 2791 complex elements measured for HV polarisation. Again, the total size of the matrix is dependent on the level of coupling between polarisations through the cross-polarisation antenna patterns. If they can be considered negligible, the J matrix can be split into three separate and independent matrices, one for each polarisation.

For the column elements ordering, it shall follow the ordering indicated below:

- The first column shall correspond to the real component of the zero baseline for the H polarisation Brightness Temperature frequencies
- The next 1395 columns shall correspond to the real components of the H polarisation Brightness Temperature frequencies
- The next 1395 columns shall correspond to the imaginary components of the H polarisation Brightness Temperature frequencies
- The next column shall correspond to the real component of the zero baseline for the V polarisation Brightness Temperature frequencies
- The next 1395 columns shall correspond to the real components of the V polarisation Brightness Temperature frequencies
- The next 1395 columns shall correspond to the imaginary components of the V polarisation Brightness Temperature frequencies
- The next 2791 columns shall correspond to the real components of the HV polarisation Brightness Temperature frequencies, with the zero baseline as the first column

The next 2791 columns shall correspond to the imaginary components of the HV polarisation Brightness Temperature frequencies, with the zero baseline as the first column.

The distribution of elements within each sub-group of 1395 columns shall follow the order described next. This ordering is based on reporting only the baselines with positive *v* coordinate and *u* positive for *v*=0:

- The *v* coordinate for the upper half of the baselines goes continuously from 0 to sqrt(3)*NEL*d, where NEL=21 and d=0.875, in incremental steps of sqrt(3)*d/2
- The *u* coordinate of the upper half of the baselines shall follow the mathematical rules defined as:
  - If *v*=0, then *u* goes from d to 24*d in incremental steps of d
  - If *v*>0 and *v*<=sqrt(3)*NEL*d/2, then *u* goes from –(NEL*d +*v*/sqrt(3)) to +(NEL*d +*v*/sqrt(3)) in incremental steps of d
  - If *v*=sqrt(3)*(NEL+1)*d/2, then *u* goes from –11*d to +11*d in incremental steps of d
  - If *v*=sqrt(3)*(NEL+2)*d/2, then *u* has the values –23*d/2, –19*d/2 to +19*d/2 in incremental steps of d and +23*d/2. Notice that the elements ±21*d/2 are not present.

- If *v*=sqrt(3)*(NEL+3)*d/2, then *u* has the values –12*d, –9*d to +9*d in incremental steps of d and +12*d. Notice that the elements ±11*d and ±10*d are not present.
- Finally, if *v*>sqrt(3)*(NEL+3)*d/2 and *v*<=sqrt(3)*NEL*d, then *u* goes from –(NEL*d – *v*/sqrt(3)) to +(NEL*d –*v*/sqrt(3)) in incremental steps of d

The order followed is shown in the next picture. For the 1395 element vector, the baselines shall be taken first from left to right, then from bottom to top. I.e. the first 24 elements are the ones with v=0 and ordered by increasing u; the next 42 elements are the ones with v=sqrt(3)*d/2 and ordered by increasing u (from negative to positive), and so on until the 1395 elements are covered.

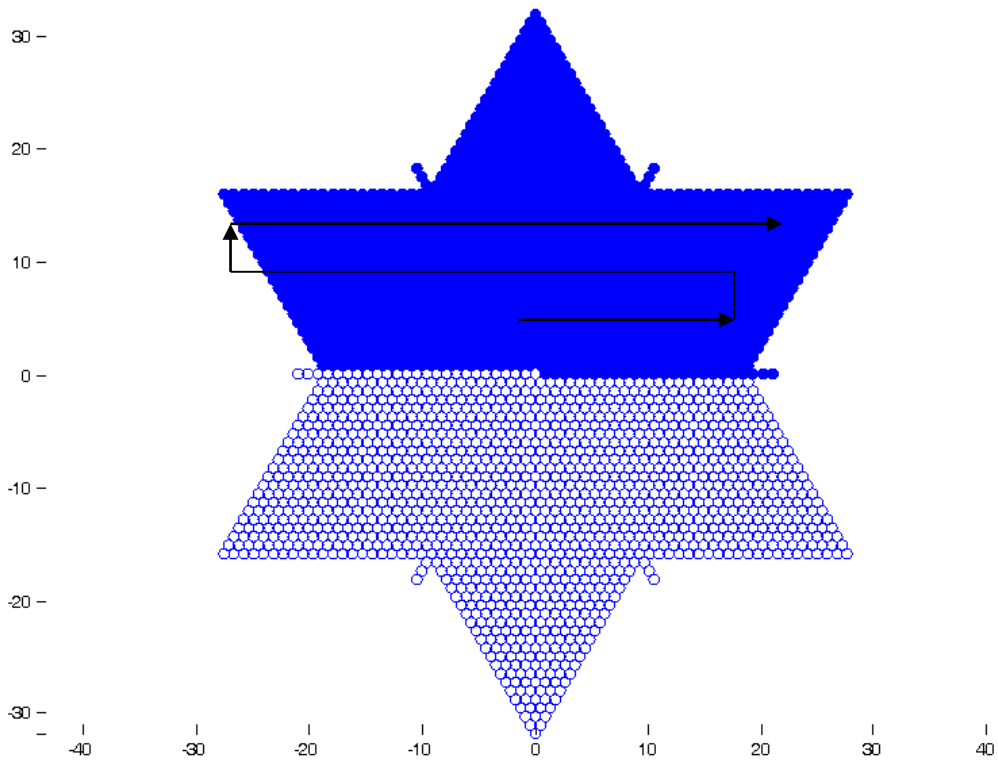

Figure 8: J Matrix Representation

For the case of HV polarisation, where the vector is 2791 elements long, the complete star must be covered. In this case, the ordering shall be similar to the one adopted above. The first element shall be the zero baseline (u=0, v=0); the next 1395 elements shall be ordered like it has been described (left to right, then bottom to top); and the remaining 1395 element shall be ordered in the same way as well, but inverting the sign of the resulting u and v coordinates (i.e. it changes to ordering from right to left, then top to bottom).

The resulting J matrix shall be inverted, making it possible to obtain the Brightness Temperature frequencies by simple multiplication of the inverted J by the L1a calibrated visibilities. It is important to define a common format so that the L1b output is coherent.

3.2.1. J Matrix Inversion

Once it has been generated, the J-matrix needs to be inverted in order to obtain $\hat{T}(u,v)$. The inversion is achieved by using the pseudo-inverse:

$$\begin{aligned} J \cdot \hat{T} &= V \\ J^* J \cdot \hat{T} &= J^* V \\ \hat{T} &= \left(J^* J\right)^{-1} J^* V \\ J^+ &= \left(J^* J\right)^{-1} J^* \end{aligned} \qquad \textit{Eq. 11}$$

J is the System Response Function expressed in the Brightness Temperatures Frequency domain (star domain). J^* is the conjugate transpose of J, and J^+ is its pseudo-inverse

The result of multiplying J^+ by the calibrated visibilities V is the brightness temperatures frequencies $\hat{T}(u,v)$, expressed in the frequency star domain.

In fact, in order to give the user more configuration flexibility to take into account e.g. possible hardware failures, the temperature frequencies are instead obtained by multiplying J^+ by WV ($\hat{T} = J^+ W V$), where W is a diagonal matrix whose entries consist of user configurable weights for each baseline. These baseline weights (whose default value is 1) are obtained from the `SM_xxxx_AUX_BWGHT_<ID>` Auxiliary Data File defined in [AD.13].

As a further step for the baseline weighting, the method described in [RD.6] is recommended for the operational algorithm. This method consists on a baseline avoidance algorithm, which will respect the format of the J+ matrix, but will take into account during the inversion process that some baselines are not desired (i.e. NIR-NIR baselines across arms and baselines across instrument hinges). This algorithm will use data from two additional auxiliary files during the J matrix inversion (BWGHT and FAIL ADF).

The baselines identified as the ones to be always removed are:

NIR-NIR baselines	Hinges baselines
01 NIR-AB-01 H --- NIR-BC-01 H	1 LCF-A-03 LCF-A-04
02 NIR-AB-01 H --- NIR-BC-01 V	2 LCF-A-09 LCF-A-10
03 NIR-AB-01 H --- NIR-CA-01 H	3 LCF-A-15 LCF-A-16
04 NIR-AB-01 H --- NIR-CA-01 V	4 LCF-B-03 LCF-B-04
05 NIR-AB-01 V --- NIR-BC-01 H	5 LCF-B-09 LCF-B-10
06 NIR-AB-01 V --- NIR-BC-01 V	6 LCF-B-15 LCF-B-16
07 NIR-AB-01 V --- NIR-CA-01 H	7 LCF-C-03 LCF-C-04
08 NIR-AB-01 V --- NIR-CA-01 V	8 LCF-C-09 LCF-C-10
09 NIR-BC-01 H --- NIR-CA-01 H	9 LCF-C-15 LCF-C-16
10 NIR-BC-01 H --- NIR-CA-01 V	
11 NIR-BC-01 V --- NIR-CA-01 H	
12 NIR-BC-01 V --- NIR-CA-01 V	

Table 3-3 - Baselines to be removed from J+

3.2.2. Implementation

This method requires to compute the *J*-matrix, whose size is much smaller than the *G*, as it merely relates the calibrated visibilities to the brightness temperatures frequencies, $\hat{T}$. The number of these frequencies is equal to the number of non-redundant baselines N_f: 1396 for H and V polarisations and 2791 for HV polarisation.

The matrix *J* is computed by using *G* to create the expected calibrated visibilities for some specific Brightness Temperatures. These specific Brightness Temperatures are computed by setting to unity each of the non-redundant baselines in the star domain and perform a normal 2D IFFT on the resulting distribution. Each computed set of Brightness Temperatures for each of the non-redundant baselines results in a complete column of the J matrix.

The method can be modelled in the following way:

- Enter a for loop for each of the non-redundant baselines, which correspond to a particular (***U,V***) position (the order to be taken is described in [AD.5])
- Using Eq. 11 an $N_T x N_T$ complex matrix is created for the u,v baselines with zero in all positions except for the (*u,v*) position where the complex number (1+i) is set.
- In H or V polarisation, the complex number (1–i) is also set in the (-*u,-v*) position, and only half of the non-redundant baselines shall be used (1396)
- In HV polarisation no other value is changed from zero, and all the non-redundant baselines shall be used (2791)
- A 2D Inverse Fast Fourier Transform is performed on the resulting $N_T x N_T$ complex matrix, which will generate a new $N_T x N_T$ complex matrix. In H or V polarisation, as the input matrix is Hermitian, the output matrix shall be real valued.
- This new $N_T x N_T$ complex matrix is ordered in vector format, zero-padded to form a $4 x N_T x N_T$ real valued vector and multiplied by *G* as shown in Figure 10. Notice that depending on the polarisation being used, the zero padding of the vector in the figure may vary (e.g. if the vector corresponds to H polarisation, the V and HV polarisation components must be filled with zeroes).
- The resulting vector of the matrix vector multiplication shall be a complete column of the J matrix applicable to the (*u,v*) baseline.

Continue the loop until all columns of *J* have been computed.

After the generation of the *J*-matrix it is needed to invert (J^+) it in order to be used in the image reconstruction module. To do the inversion Eq. 11 will be used and then the module will generate the corresponding ADF file.

The result of multiplying J^+ by the calibrated visibilities *V* is the brightness temperatures frequencies $\hat{T}(u,v)$, expressed in the frequency star domain.

The calibrated visibilities must be ordered in a very precise way, in order to match the way in which the *J*- and *G*-matrices were generated. This ordering is described in chapter 4.18.3 of [AD.5]. Visibilities for H and V polarisations in two consecutive integration times must be used in dual polarisation mode, while visibilities for H, V and HV polarisation in two consecutive integration times must be used in full

polarisation mode. For a comprehensive analysis on the HV visibilities ordering and location, please refer to [RD.2].

In addition, the new Baselines Avoidance Algorithm has been implemented in L1OP. This file takes into account baselines affected by external contamination and which are not desired in the reconstruction process, and filters them out during the inversion process. For detailed information, please refer to [RD.6].

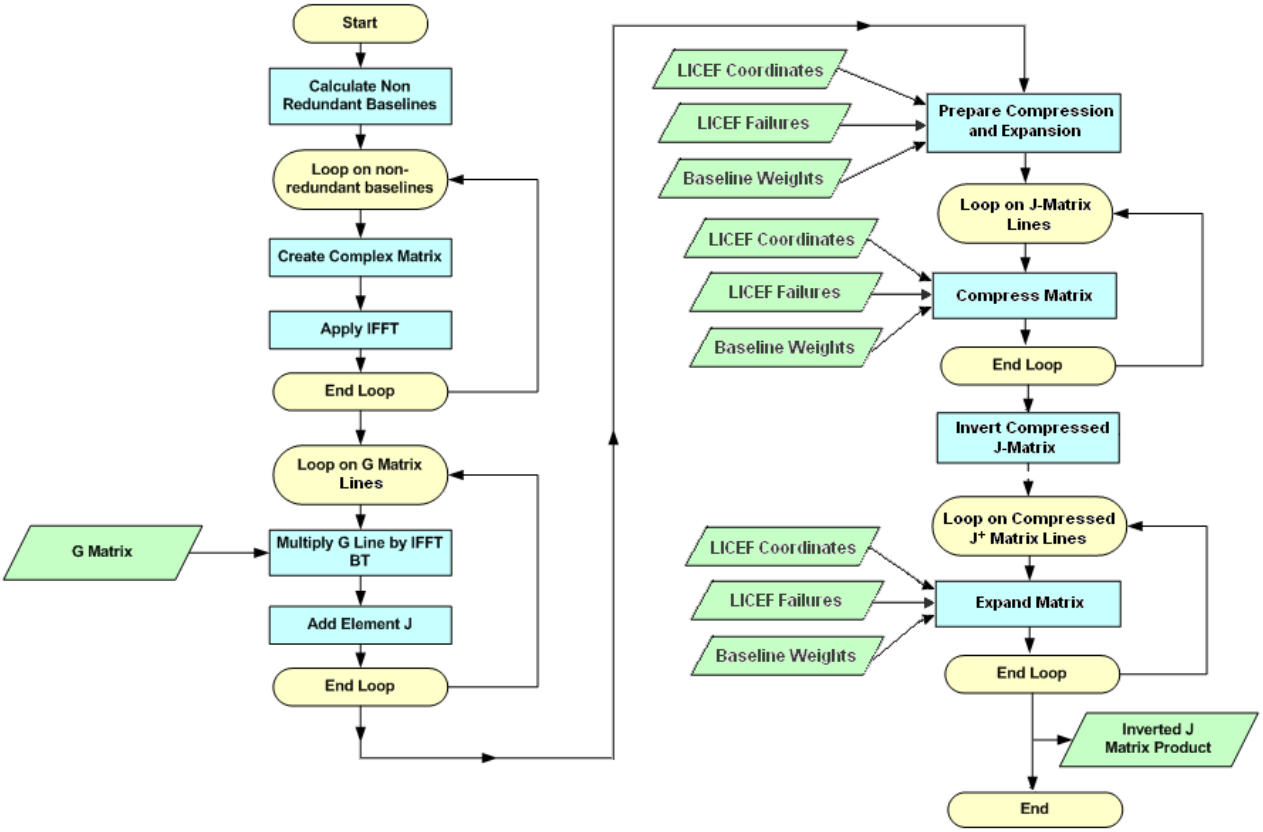

Figure 9: J-matrix Generation and Inversion Flow

3.2.2.1. Inputs

- *G*-matrix auxiliary file (SM_xxxx_AUX_GMAT__<ID>)
- Baseline Weights auxiliary file (SM_xxxx_AUX_BWGHT_<ID>)
- Element Failure auxiliary file (SM_xxxx_AUX_FAIL__<ID>)

3.2.2.2. Outputs

- Inverted J-matrix auxiliary file (SM_xxxx_ AUX_JMAT__<ID>)

3.2.2.3. List of Variables

The following table describes the variables used in the subsequent implementation section. Variables are listed as input, local and output (I, L, O). The *Size* column indicates the number of elements constituting that variable, and NOT the size of the variable in bytes (this information can be taken from the *Type* column).

Variable name	Description	Definition	Type	Class	Unit	Size
gmatrix_filename	*G*-matrix ADF filename	N/A	char	I	N/A	Pointer
coord_matrix	Matrix ready to apply IFFT	Eq. 4		L		[128] x [128]
coord_matrix_ifft	Recovered Matrix	N/A	real	L		[128] x [128]
J_mat_column	*J*-matrix in vector column		double	L		15996
Jmatrix	Complete *J*-matrix	[AD.13]	double	L		[15996] x [11164]
Jmatrix_inv	Inverted *J*-matrix (J^{+})	Eq. 11	double	O	N/A	[15996] x [11164]

Table 3-4: J Matrix Variable List

3.2.2.4. Implementation details

The function ***generate_jmatrix*** is responsible for the generation of a *J*-matrix already inverted. It receives as input a *G*-matrix created before. The output will be a *J*-matrix already inverted and ready for the image reconstruction module.

```
error = getUVBaselines(u, v);
error = getNRBaselines(u, v, nr_baselines);
for(i=0;i!=nr_baselines.count;++i){
   error = computeCoordinates(u[i], v[i] ,coord_matrix_real, coord_matrix_img);
   /*Compute IFFT using fftw_plan_dft_2d function*/
   error = applyIFFT(coord_matrix, coord_matrix_ifft);
   error = multiplyIFFTGmat(gmatrix, coord_matrix_ifft, j_mat_column);
   jmatrix[0][n] = j_mat_column;
}
error=invertJmat(jmatrix, jmatrix_inv);
```

The first thing to do is to obtain the non-redundant baselines, using the (u,v) coordinates The result will be 1395 (u,v) coordinates forming the star domain present in Figure 8.

The function starts to invoke the ***compute_coordinates*** method to build the complex matrix for the u and v baselines with zero in all positions except in one position (where 1+i is set). It is needed to set to one the position (1-i), in order to produce a hermitian matrix. This will generate two 128 x 128 matrices, one with the real part (set to 1 and -1) and other with the imaginary part (set to i and -i) ready to apply the IFFT. In full polarization the entire star must be covered, then it will not be only 1395 baselines but 2791 complex values, instead of real values.

The following code presents the ***getUVBaselines*** function. It is implemented based on Eq. 4. It computes a rectangular matrix with the coordinates of the (u,v) distribution in the frequency domain.

```
for (i=0;i!=N-1;++i){
   for (j=0;j!=N-1;++j){
      if (i > j){
            ii = i-N; jj = j;
            if ((2*i+j-N) < 0){ ii = i;   jj = j;}
            if ((i+2*j-2*N) > 0){ ii = i-N; jj = j-N;}
      }else{
            ii = i; jj = j-N;
            if ((i+2*j-N) <= 0){ ii = i;   jj = j;}
            if ((2*i+j-2*N) >= 0){ ii = i-N; jj = j-N;}
      }
        if (i > 0){ U(j,N-i) = (jj + 0.5*ii)*d;}
        if (i == 0) U(j,i) = (jj + 0.5*ii)*d;
        V(N-j,i) = (0.5*sqrt(3)*ii)*d;
    }
}
```

The ***apply_ifft*** method will use the fftw library methods. At this level we will use the function fftw_plan_dft_2d. It receives as arguments the number of lines and columns, the source matrix and the FFT method. The type of the source and result matrix must be fftw_complex and the memory allocation must be done by the fftw methods. The resulting IFFT values must not be normalized.

After the IFFT vectors are calculated it is needed to transform them to a column vector to be multiplied with the *G*-matrix. The result of this operation is one column of the J matrix. In order to optimize the operation the method ***multiply_ifft_gmat*** will only load one line of the *G*-matrix and multiply it by all the ifft vectors.

```
m = gmatrix_rows; n = gmatrix_columns;
for(int i=0; i!=gmatrix_rows;++i){
   error = getGLine(i, g_mat_line);
   //Dual Pol
   for(int j=0;j != NRB, ++j){
      j_matrix[i][j] = ddot_(&line_size, g_mat_line, &step, ifft_vector_real[j],&step);
      j_matrix[i][j+1395] = ddot_(&line_size, g_mat_line, &step, ifft_vector_imag[j],
&step);
   }
   //Full Pol
   for(int j=0;j != NRB, ++j){
      j_matrix[i][j] = ddot_(&line_size, g_mat_line, &step, ifft_vector_real[j],&step);
      j_matrix[i][j+2791] = ddot_(&line_size, g_mat_line, &step, ifft_vector_imag[j],
&step);
   }
}
```

The result J Matrix will have the structures presented in the picture below.

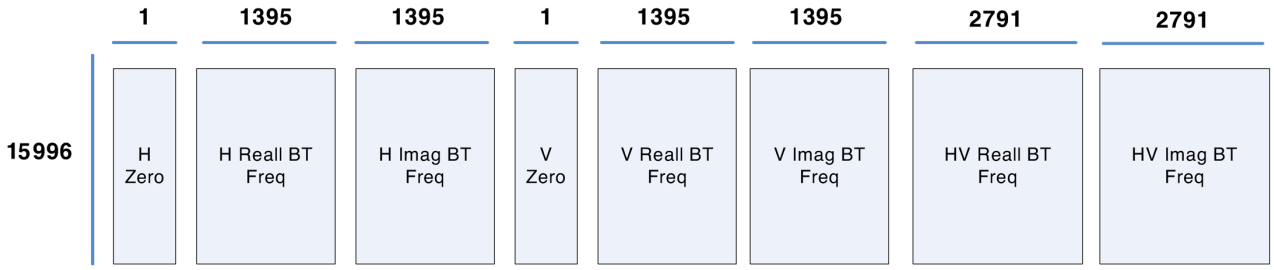

Figure 10: J Matrix Structure

The ***invert_j_matrix*** method uses some LAPACK methods to invert the J matrix generated. The inversion is performed using SVD methods. After the Singular Value Decomposition of J is performed ($J=UxSxV^T$), the pseudo-inverse J^+ is easily computed doing $J^+=V^TxS^{-1}xU$.

```
dgesvd_(&jobu, &jobvt, &ncols, &nrows, matrix, &ldmatrix, s, u, &ldu, vt, &ldvt, work,
&lwork, &info);

for (i=0;i<ncols;i++)

   {matrix[i][i] = 1./s[i];}

dgemm_(&transa, &transb, &nrows, &ncols, &nrows, &alfa, vt, &nrows, matrix, &ncols,
&beta, svd_matrix, &nrows);

dgemm_(&transa, &transb, &nrows, &ncols, &ncols, &alfa, svd_matrix, &nrows, u, &ncols,
&beta, matrix, &nrows);

jmatrix_inv=matrix;
```

In order to confirm that the inversion values are in line with the expected it is good to check the output of the dgesvd_ function. The rank, or number of Singular Values "significantly" different from zero, must be exactly the number of columns (2791x4). This is easily seen in a representation of the SVD values like in the next figure, by verifying that there are no magnitude jumps which could indicate duplication of lines in previous computations. This method is mentioned here because it has been a great help during the prototype implementation.

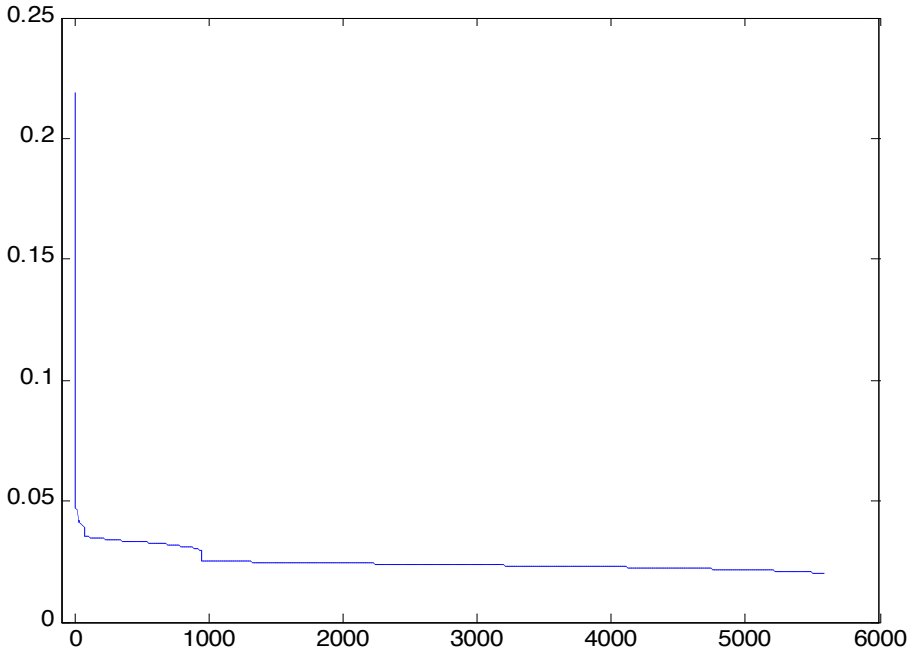

Figure 11: SVD Output Values

It is very important to store in the J^{+}-matrix header the correlator layer (Nominal or Redundant) that was active when the FWF shape, used to compute the *G*-matrix, was measured. This value can be

retrieved from the FWF shape product header, and it is required to determine which data can be reconstructed with the J+ matrix product.

3.3. AUX_FTT

This is a specific module which generates the FTT ADF based on External Target observation data. Such generation is based on consecutive scenes taken while observing a relatively Flat portion of the Sky, and the instrument measurements together with other L1OP generated data shall be stored in the ADF for later use during nominal processing.

This module shall select a sequence of continuous external target scenes (typically 500, but value shall be configurable) whose expected Sky image RMS is lower than a certain configurable value. The RMS values shall be taken from the Galaxy Map ADF, where they have been computed beforehand.

Once the scenes are selected, this module shall perform an averaging of all the L1a calibrated visibilities, producing 3 averaged output scenes: one for H polarisation, one for V polarisation and another for HV polarisation (this last only if measuring in full pol mode, otherwise it shall be set to 0). Furthermore, according to the Baseline Based Algorithm for the Flat Target Transformation, [RD.5], this module also computes the average physical temperature for the 72 receivers.

Additionally, it shall also average the NIR Brightness Temperatures for all the scenes, and the physical temperature of the receivers.

Besides this data averaging, the processing module shall also compute additional visibilities using the best instrument modelling available (i.e. the latest *G*-matrix). One set of visibilities for the expected Sky observed, and another for a uniform 1K scene in the whole unit circle.

For this purpose it shall compute the expected Sky Brightness Temperature in the Antenna Plane being observed by the instrument during the scene averaging. This information shall be computed using the instrument pointing and the Galaxy Map BT distribution and the average value for each polarization is also stored for the computation of the scaling factors to be applied during the science processing.

The 1K scene is self-explanatory, as it shall always be 1 regardless of the ξ-η coordinates.

These two BT distributions (in all available polarisations) shall be multiplied by the *G*-matrix, obtaining the expected visibilities as output. As part of this output, the expected NIR BT shall also be obtained. As these visibilities are computed using the *G*-matrix, their sizes shall be the following ones:

- V_{SkyFFT} shall contain 3 real elements plus 2346 complex elements for H or V polarisation, and 3303 complex elements for HV polarisation
- $V_{UniformFFT}$ shall contain 3 real elements plus 2346 complex elements for H or V polarisation, and 3303 complex elements for HV polarisation

V_{FFT} shall contain 3 real elements plus 2556 complex elements for H or V polarisation, and 3 real elements plus 3*2556 complex elements for HV polarisation. These quantities shall be reduced to the same amounts as the previous values by discarding the cross-polar measurements of LICEF-NIR elements in dual polarisation, and by data combination as described in [RD.2] in the case of full pol scenes.

4. L1OP ADF DESCRIPTION

The following table summarises the origin of the data contained in each ADF, specific tools used in its generation and special procedures followed (if any):

Table 4-1: Generation Procedures Auxiliary Data Files

Type of Data	Origin of Data	Specific Tools	Procedure
AUX_APDL__ AUX_APDS__	Blackmann function equation Eq. 17 of DPM L1C	None	Generated manually by DEIMOS. Fixed file, generated only once.
Best Fit Plane (AUX_BFP)	On-ground measurement data provided by EADS CASA Espacio with MIRAS Database v2.2 In-orbit measurements provided by CESBIO (F. Cabot). Updated with values provided on 08/2013. [RD.18]	None	Generated manually by DEIMOS.
Bistatic Scattering Coefficients (AUX_BSCAT)	Look-Up-Table provided by IFREMER.	None	Generated manually by DEIMOS. Fixed file so it had to be generated only once.

Type of Data	Origin of Data	Specific Tools	Procedure
IERS Bulletin B File	File provided by SMOS FOS	None	None
Baseline Weights (AUX_BWGHT)	Suppressed baselines defined during KP3 (weight set to zero) NIR-LICEF baselines provided by OBS-MIP (E. Anterrieu) Updated to discard BCH01xBCV01 baselines (since NIR BC is now in failure)	None	Generated manually by DEIMOS.
Discrete Global Grid (AUX_DGG)	ISEA aperture 4, resolution 9 global hexagonal grid (4H9), generated by DGGRID GETASSE30 used for the altitude computation of each grid cell	DGGRID Software (http://webpages.sou.edu/~sahrk/dgg/dggrid/dggrid.html) Modified DGGRID instance for binning GETASSE30 DEM into ISEA	Generated by DEIMOS using the available tools
Failing Components Table (AUX_FAIL)	NIR AB and BC set to failure at Cal Team recommendation.	None	Generated manually by DEIMOS.

Type of Data	Origin of Data	Specific Tools	Procedure
Instrument Response Matrix	G-Matrix, computed by CESBIO according to the procedure in Section 3.1. Hexagonal coordinates, Full Cross-Polar data. Updated to remove NIR-NIR correlations for HV (cross-coupling correction already applied at L1a) Updated to substitute the Antenna Patterns in the first three rows of the Dual Pol section by the weighted LICEF Antenna Pattern Average ([RD.20] and [RD.21])	CESBIO breadboard software (L1a2b)	Specified in Section 3.1.
Instrument Response Matrix for ALL-LICEF mode	G-Matrix, computed by CESBIO according to the procedure in Section 3.1. Same procedure as for default G-Matrix but replacing the first three rows NIR Aps with average LICEF patterns	CESBIO breadboard software (L1a2b)	Specified in Section 3.1.4.

Type of Data	Origin of Data	Specific Tools	Procedure
Inverse Instrument Response Matrix	J-Matrix, computed by CESBIO according to the procedure in Section 3.2. Hexagonal coordinates, Full Cross-Polar data. Updated to J-matrix provided on 08/2013, removing a unwanted NIRxNIR correlation line. Updated to substitute the Antenna Patterns in the first three rows of the Dual Pol section by the weighted LICEF Antenna Pattern Average ([RD.20] and [RD.21])	CESBIO breadboard software (L1a2b)	Specified in Section 3.2.
Inverse Instrument Response Matrix for ALL-LICEF mode.	J-Matrix, computed by CESBIO according to the procedure in Section 3.2. Same procedure as for default J-Matrix but inverted from G-Matrix for ALL-LICEF mode.	CESBIO breadboard software (L1a2b)	Specified in Section 3.2.

Type of Data	Origin of Data	Specific Tools	Procedure
Galaxy L-band Map (AUX_GALAXY)	Values of the first 4 layers have been taken directly from the map produced by ESA (N. Floury, 15-01-2008 v2.1) Final two layers representing the NIR expected measurements and RMS values that are used in NIR calibration and FTT were provided by EADS CASA Espacio. Updated with latest map provided by Nicolas Floury with corrections to the HI line position and coordinate mapping.	Matlab script developed by DEIMOS.	Generated manually by DEIMOS using available tool.

Type of Data	Origin of Data	Specific Tools	Procedure
Receivers Characterisation (AUX_LCF)	On-ground measurement data provided by EADS CASA Espacio with MIRAS Database v2.2 and updated with latest LICEF antenna model coefficients. Updated antenna phases according to UPC TN [RD.7] Updated L1 and L2 values according to UPC recommendation [RD.14] Updated with the Gkj correction factor Updated with new Front End Losses factors for the ALL-LICEF mode ([RD.21]) Updated with Full-Polarisation relative phases computed during IVT ([RD.22]) Added independent Gkj factors for NIR and ALL-LICEF modes	None	Generated manually by DEIMOS.

Type of Data	Origin of Data	Specific Tools	Procedure
Land/Sea Mask (AUX_LSMASK)	USGS LandSea Mask (http://edc2.usgs.gov/1KM/land_sea_mask.php) binned to ISEA 4H9 grid MERIS Hierarchical Coastline data provided by Brockman Consulting	Modified DGGRID instance for binning USGS LandSea Mask into ISEA Ad-hoc C99 tool created to combine USGS binning and MERIS coastline data into final binary file.	Generated by DEIMOS using the available tools (first USGS binning, then adding the hierarchical coastlines)
L1C Pixel Mask (AUX_MASK)	List of pixels to be stored in SM or OS products was provided by L2 teams	Ad-hoc C99 tool created to combine OS and SM pixel lists into final binary file.	Generated by DEIMOS using the available tool
Mispointing Angles (AUX_MISP)	On-ground measurement data provided by EADS CASA Espacio with MIRAS Database v2.2 Updated with values provided on 08/2013. The rotation coordinates were corrected to be consistent with new BFP computed by CESBIO.	None	Generated manually by DEIMOS.

Type of Data	Origin of Data	Specific Tools	Procedure
Moon Brightness Temperature Map Model (AUX_MOONT)	Data currently not available	None	Generated manually by DEIMOS with placeholder values.

Type of Data	Origin of Data	Specific Tools	Procedure
NIR Characterisation tables (AUX_NIR)	On-ground measurement data provided by EADS CASA Espacio with MIRAS Database v2.2 Data refined with latest NIR antenna model evolution from HUT (J. Kainulainen) [RD.10] Updated L1 and L2 values according to UPC recommendation [RD.14] Updated NIR response coefficients according to HARP TN [RD.15] Updated to support fixed Tna0 and Tnr0, including propagation coefficients ([RD.26]) Updated to include new Tp7 latency correction parameter ([RD.25])	None	Generated manually by DEIMOS.

Type of Data	Origin of Data	Specific Tools	Procedure
PLM Characterisation Table (AUX_PLM)	On-ground measurement data provided by EADS CASA Espacio with MIRAS Database v2.2 Changed referential for xi axis, to be consistent with G/J+ matrices produced by CESBIO. Updated with LICEF TA average weighting factors ([RD.21])	None	Generated manually by DEIMOS.
PMS Characterisation tables (AUX_PMS)	On-ground measurement data provided by EADS CASA Espacio with MIRAS Database v5.1 Updated with new Double Exponential coefficients for Heater Delay correction ([RD.23]) Updated Gains Sensitivities to latest values provided by BEC in 2016 ([RD.24])	None	Generated manually by DEIMOS.

Type of Data	Origin of Data	Specific Tools	Procedure
RFI sources Map (AUX_RFI)	Data currently not available (dummy file)	None	Generated manually by DEIMOS with placeholder values.
RFI Sources List (AUX_RFILIST)	File provided by L2 contractor (ARRAY) Computed with methods described in [RD.17]	None	None.
Relevant S-parameters of MIRAS (AUX_SPAR)	On-ground measurement data provided by EADS CASA Espacio with MIRAS Database v2.2 Updated CAS factors to UPC latest computed values [RD.14] Updated with CAS factors optimized for use with fixed Tna/Tnr and new L1/L2 values ([RD.26])	None	Generated manually by DEIMOS.
Sun Brightness Temperature Map Model (AUX_SUNT)	Data currently not available	None	Generated manually by DEIMOS with placeholder values.
Reference Orbit Scenario File	File provided by SMOS FOS	None	None

Type of Data	Origin of Data	Specific Tools	Procedure
Average Antenna Patterns (AUX_PATT))	On-ground measurement data provided by EADS CASA Espacio with MIRAS Database v2.2 Updated to include individual backlobe patterns and resampled to 196x196 ([RD.27])	None	Generated manually by DEIMOS using CESBIO inputs.
Fringe Wash Function Coefficients file	Approximation of the FWF shape, computed by DEIMOS from 2010 data and used in the computation of the System Response	G-Matrix generator	Generated by DEIMOS with G-Matrix generator
Static Fresnel Model	CESBIO implementation of the model for the maximum ellipse extension of the Earth disc	CESBIO breadboard software (L1a2b)	Generated manually by DEIMOS using CESBIO data

5. AUXILIARY DATA FILES

The following tables identify the ADFs ingested by L1OP v7.2.0 and provide relevant information about these files. A specific statement is included about the applicability of each file to the Launch Baseline or not, depending on whether the file is ready to be used.

As of post-Launch, no FTTx are provided in the ADF TDS, as the formal baseline is available from other sources within DPGS (as is the case for other operational products like the ANIR, which are not considered ADF and thus not provided in this TDS).

Despite the fact that all the files have ".EEF" extension, some of them are pure XML files instead of "Hybrid" composed of an XML Header and a Binary Data Block. Tables 4 and 5 contain a column describing the internal format of the file, which can be:

EEF – Hybrid Files containing an XML Header and a Binary Data Block;

XML - Pure XML Files, following the Earth Explorer File Format Standard.

The files already with code "OPER" were provided by the DPGS operational team, based on previous deliveries by the L1OP team ([RD.19]).

Table 5-1: List of Auxiliary Data Files

Type of Data	Description	File Name	Size	Format
Apodisation Window Coefficients	Defines the apodisation function coefficients over the frequency domain coordinates (U,V) for the Blackman Window. Launch Baseline	SM_OPER_AUX_APDL___20050101T000000_20500101T000000_300_003_3.EEF SM_OPER_AUX_APDS___20050101T000000_20500101T000000_300_003_3.EEF	216 028 216 027	XML

Type of Data	Description	File Name	Size	Format
Best Fit Plane	Euler Rotation Angles between Antenna Reference Frame and Best-Fit Plane. Values provided on 08/2013. [RD.18]	SM_OPER_AUX_BFP____20050101T000000_20500101T000000_340_004_3.EEF	2 559	XML
Bistatic Scattering Coefficients	Bistatic Scattering Coefficients used for removing Sun Glint effects. Look-Up-Table provided by IFREMER. Launch Baseline	SM_OPER_AUX_BSCAT__20050101T000000_20500101T000000_300_003_3.EEF	832 352	EEF
IERS Bulletin B File	Bulletin B Earth Orientation parameters, linking UTC time to UT1, TAI and GPS time. Generated by IERS File provided for completeness and reproduction of L1OP TDS results. L1OP is not the official provider of this file. Post-Launch Baseline	SM_TEST_AUX_BULL_B_20100103T000000_20100201T235959_100_001_3.EEF SM_TEST_AUX_BULL_B_20100202T000000_20100301T235959_100_001_3.EEF SM_TEST_AUX_BULL_B_20100702T000000_20100801T235959_100_001_3.EEF SM_TEST_AUX_BULL_B_20100802T000000_20100901T235959_100_001_3.EEF SM_OPER_AUX_BULL_B_20110102T000000_20110201T235959_120_004_3.EEF SM_OPER_AUX_BULL_B_20110602T000000_20110701T235959_120_004_3.EEF SM_TEST_AUX_BULL_B_20120602T000000_20120701T235959_120_001_3.EEF SM_TEST_AUX_BULL_B_20120702T000000_20120801T235959_120_001_3.EEF	17033 16553 17276 17167 17221 17304 17331 17584	EEF

Type of Data	Description	File Name	Size	Format
Baseline Weights	Baseline weights used during Image Reconstruction to alter the relative weight of certain baselines First in-orbit characterisation of NIR-LICEF weights, plus hinge baselines and NIR-NIR baselines across arms are suppressed (weight set to 0) Post-Launch (KP3) Baseline. The baseline formed by NIR AB has also been removed. Removed baseline BCH01xBCV01, since NIR BC is now in failure.	SM_OPER_AUX_BWGHT__20050101T000000_20500101T000000_340_006_3.EEF	337 103	XML

Type of Data	Description	File Name	Size	Format
L1 Algorithm Configuration File	Unified L1 algorithm configuration file, containing L1 science and calibration configurations. Post-Launch Baseline. Adapted sequence consolidation for L1OP test campaign. Updated with new thresholds for RFI flagging Updated with new RFI circle computation parameters [RD.13] Updated with new ALL-LICEF mode switch Updated PMS External Minimum Epochs to 1, to trigger LFE computation Updated with new thresholds for RFI contamination flagging, introduced in latest version of RFI flagging note ([RD.13]) Updated with flags to control fixed Tna0/Tnr0 and Tp7 latency correction ([RD.25 and 26])	SM_TEST_AUX_CNFL1P_20050101T000000_20500101T000000_720_001_0.EEF	15817	XML

Type of Data	Description	File Name	Size	Format
Discrete Global Grid	ISEA aperture 4, resolution 9 global hexagonal grid, containing geodetic coordinates (lat-lon-alt) of all pixels. Launch Baseline	SM_OPER_AUX_DGG____20050101T000000_20500101T000000_300_003_3.EEF	41 943 320	EEF
Failing Components Table	Failing components table set to no failures in any element, except for NIR-AB, as per QWG-3 recommendation. Post-Launch Baseline. NIR BC is now set to be in failure, by Cal Team recommendation.	SM_OPER_AUX_FAIL___20050101T000000_20500101T000000_300_004_3.EEF	51 275	XML

Type of Data	Description	File Name	Size	Format
Galaxy L-band Map	Map of the Galaxy Brightness Temperatures containing 6 layers of721x1441 elements. Values of the first 4 layers have been taken directly from the map produced by ESA (N. Floury), plus two additional layers representing the NIR expected measurements and RMS values that are used in NIR calibration and FTT. All values contain the latest baseline available from ESA, including cross-polar measurements above -20º declination. Launch Baseline. Data Updated with latest Sky Map recomputed by Nicolas Reul, fixing problems found in HI line and grid coordinates interpolation. Provided by ESA.	SM_OPER_AUX_GALAXY_20050101T000000_20500101T000000_300_004_3.EEF SM_OPER_AUX_GALNIR_20050101T000000_20500101T000000_300_003_3.EEF	16 623 376 8 311 688	EEF

Type of Data	Description	File Name	Size	Format
Instrument Response Matrix	G-Matrix, computed by CESBIO according to the procedure in Section 3.1. Hexagonal coordinates, Full Cross-Polar data. Updated to remove NIR-NIR correlations for HV (cross-coupling correction already applied at L1a). Operational version delivered by IDEAS ([RD.19]).	SM_OPER_MIR_GMATD__20100101T144504_20100101T162500_600_007_3.EEF	19664074752	EEF
Instrument Response Matrix for ALL-LICEF mode	G-Matrix, computed by CESBIO according to the procedure in Section 3.1.4. Updated to substitute the Antenna Patterns in the first three rows of the Dual Pol section by the weighted LICEF Antenna Pattern Average ([RD.20] and [RD.21])	SM_TEST_MIR_GMATD__20100101T144504_20100101T162500_700_001_3.EEF	19664074752	EEF

Type of Data	Description	File Name	Size	Format
Inverse Instrument Response Matrix	J-Matrix, computed by CESBIO according to the procedure in Section 3.2. Hexagonal coordinates, Full Cross-Polar data. Updated to version delivered on 08/2013, fixing remaining NIRxNIR baselines. Operational version delivered by IDEAS ([RD.19]).	SM_OPER_MIR_JMATD__20100101T144504_20100101T162500_600_007_3.EEF	1428634752	EEF
Inverse Instrument Response Matrix for ALL-LICEF mode	J-Matrix, computed by CESBIO according to the procedure in Section 3.2., from G-Mtraix for ALL-LICEF mode. Updated to substitute the Antenna Patterns in the first three rows of the Dual Pol section by the weighted LICEF Antenna Pattern Average ([RD.20] and [RD.21])	SM_TEST_MIR_JMATD__20100101T144504_20100101T162500_700_001_3.EEF	1428634752	EEF

Type of Data	Description	File Name	Size	Format
Receivers Characterisation	Receivers characterisation (ohmic efficiency and absolute phase). First version of in-orbit characterised antenna efficiency values after changing the LICEF antenna model. Post-Launch Baseline Updated antenna phases according to UPC TN [RD.7] Updated L1 and L2 values according to UPC recommendation [RD.14] Updated with the Gkj correction factor Updated with new Front End Losses factors for the ALL-LICEF mode ([RD.21]) Updated with Full-Pol receiver phases from [RD.22] Added new gkj factors for NIR and ALL-LICEF independently	SM_TEST_AUX_LCF____20050101T000000_20500101T000000_720_001_0.EEF	94378	XML
Land/Sea Mask	ADF extracted from combining the USGS Land-Sea mask and ISEA grid. Launch Baseline	SM_OPER_AUX_LSMASK_20050101T000000_20500101T000000_300_003_3.EEF	15 728 820	EEF

Type of Data	Description	File Name	Size	Format
L1C Pixel Mask	ADF extracted from combination of Land-Sea Mask flags. This mask contains the latest baseline agreed with L2 teams, including the 200km overlap over coastlines. Launch Baseline	SM_OPER_AUX_MASK___20050101T000000_20500101T000000_300_002_3.EEF	13 107 370	EEF
Mispointing Angles	ADF containing measured or estimated mispointing angles between the Star Tracker unit and the PLM Launch Baseline	SM_OPER_AUX_MISP___20050101T000000_20500101T000000_300_004_3.EEF	2 858	XML
Moon Brightness Temperature Map Model	Moon Brightness Temperature measurements, to be used only for reprocessing. ADF currently incomplete. Launch Baseline	SM_OPER_AUX_MOONT__20050101T000000_20500101T000000_300_002_3.EEF	2 679	EEF

Type of Data	Description	File Name	Size	Format
NIR Characterisation tables	NIR characterisation table. All values measured on-ground have been incorporated into this baseline Fourth version of in-orbit characterised sensitivity values, including new NIR drift parameters. Post-Launch Baseline Updated L1 and L2 values according to UPC recommendation [RD.14] Updated NIR response coefficients according to HARP TN [RD.15] Updated to support fixed Tna0/Tnr0 and Tp7 latency correction ([RD.25 and 26])	SM_TEST_AUX_NIR____20050101T000000_20500101T000000_720_001_0.EEF	15874	XML

Type of Data	Description	File Name	Size	Format
PLM Characterisation Table	Parameters calibrated on-ground referent to elements of the PLM. Version 300_005 and onwards must be used with in-orbit data due to the differences in central frequency. Version 600 contains new antenna pattern renormalisation factors. Post-Launch Baseline Changed referential for xi axis, to be consistent with G/J+ matrices produced by CESBIO. Updated with LICEF TA average weighting factors ([RD.21])	SM_TEST_AUX_PLM____20050101T000000_20500101T000000_700_002_0.EEF	47012	XML

Type of Data	Description	File Name	Size	Format
PMS Characterisation tables	PMS characterisation table, computed on-ground. Second Order Sensitivities have been set to zero according to KP2 recommendation. Version 600 contains new Receiver Noise Temperature fields from original MIER measurements. Post-Launch Baseline PMS Gain Sensitivities updated to latest values provided by BEC in 2016 ([RD.24]) PMS Heater Double Exponential correction coefficients added	SM_TEST_AUX_PMS____20050101T000000_20500101T000000_711_002_0.EEF	166 863	XML
RFI sources Map	ADF containing TRUE values for those pixels that are expected to be affected by RFI. Issue 2 is filled completely with zeros. Launch Baseline	SM_OPER_AUX_RFI____20050101T000000_20500101T000000_300_003_3.EEF	13 107 370	EEF

Type of Data	Description	File Name	Size	Format
RFI Sources List	ADF containing the list of global RFI sources (position, expected strength and applicable flags during L1 processing) Third operational file provided by L2 contractor, contains all RFI sources to be flagged and none to be mitigated. Post-Launch Baseline Updated values for monthly detected RFIs. Computed with methods described in [RD.17]	SM_TEST_AUX_RFILST_20100101T000000_20100131T235959_100_016_3.EEF	180365	XML
		SM_TEST_AUX_RFILST_20100201T000000_20100228T235959_100_016_3.EEF	195880	
		SM_TEST_AUX_RFILST_20100701T000000_20100731T235959_100_016_3.EEF	293250	
		SM_TEST_AUX_RFILST_20110101T000000_20110131T235959_100_016_3.EEF	274525	
		SM_TEST_AUX_RFILST_20110501T000000_20110531T235959_100_016_3.EEF	316255	
		SM_TEST_AUX_RFILST_20110601T000000_20110630T235959_100_016_3.EEF	328560	
		SM_TEST_AUX_RFILST_20120701T000000_20120731T235959_100_016_3.EEF	304485	
		SM_TEST_AUX_RFILST_20120901T000000_20120930T235959_100_016_3.EEF	292715	

Type of Data	Description	File Name	Size	Format
Relevant S-parameters of MIRAS	Noise distribution networks and switch S-parameters characterisation. NDN data has been filled with complete data from EADS CASA Espacio with the full S-parameters and corrections from UPC. Switch data has been filled using EADS CASA Espacio measurements. Third in-orbit characterisation of CAS correction factors, applicable to different dates. Post-Launch Baseline Updated CAS factors to UPC latest computed values [RD.14] Updated CAS factors to support fixed Tna /Tnr ([RD.26])	SM_TEST_AUX_SPAR___20050101T000000_20100111T120700_340_013_0.EEF SM_TEST_AUX_SPAR___20100111T120700_20110112T091500_340_014_0.EEF SM_TEST_AUX_SPAR___20110112T091500_20500101T000000_340_015_0.EEF	1429532 1429532 1429532	XML
Sun Brightness Temperature Map Model	Sun Brightness Temperature measurements, to be used only for reprocessing. ADF currently incomplete. Launch Baseline	SM_OPER_AUX_SUNT___20050101T000000_20500101T000000_300_002_3.EEF	2 678	EEF

Type of Data	Description	File Name	Size	Format
Reference Orbit Scenario File	Reference orbit description, linking UTC time to orbit time. Generated using EE CFI Function. File provided for completeness and reproduction of L1OP TDS results. L1OP is not the official provider of this file. Post-Launch Baseline	SM_OPER_MPL_ORBSCT_20091102T031142_20500101T000000_360_001_1.EEF	14 128	XML
Average Antenna Patterns	Post-Launch baseline for Antenna Patterns, including corrected xi-eta coordinates annotation and latest averaging and normalization algorithm using only 69 antennas (not duplicating NIR-LICEF patterns). Post-Launch Baseline Updated with individual backlobes. All patterns now in 196x196 resolution.	SM_TEST_AUX_PATT___20050101T000000_20500101T000000_720_001_0.EEF	1067672456	EEF
Static Fresnel Map	Fresnel Map for all possible Earth pixels	SM_TEST_AUX_FRSNEL_20050101T000000_20500101T000000_720_001_0.EEF	1229312	EEF

Type of Data	Description	File Name	Size	Format
Fringe Wash Functions coefficients file	Approximation of the FWF shape, computed by DEIMOS from 2010 data and used in the computation of the System Response	SM_TEST_MIR_AFWD1A_20100202T144510_20100202T162359_600_001_0.EEF	9087	EEF

6. ANNEX: ADF SET PACKAGE CONTENTS

```
data/adf-dpgs:
SM_OPER_AUX_APDL___20050101T000000_20500101T000000_300_004_3.EEF
SM_OPER_AUX_APDS___20050101T000000_20500101T000000_300_004_3.EEF
SM_OPER_AUX_BFP____20050101T000000_20500101T000000_340_004_3.EEF
SM_OPER_AUX_BSCAT__20050101T000000_20500101T000000_300_003_3
SM_OPER_AUX_BULL_B_20110102T000000_20110201T235959_120_004_3
SM_OPER_AUX_BULL_B_20110302T000000_20110401T235959_120_004_3
SM_OPER_AUX_BULL_B_20110502T000000_20110601T235959_120_004_3
SM_OPER_AUX_BULL_B_20110602T000000_20110701T235959_120_004_3
SM_OPER_AUX_BULL_B_20120602T000000_20120701T235959_120_001_3
SM_OPER_AUX_BULL_B_20120702T000000_20120801T235959_120_001_3
SM_OPER_AUX_BWGHT__20050101T000000_20500101T000000_340_006_3.EEF
SM_OPER_AUX_DGG____20050101T000000_20500101T000000_300_003_3
SM_OPER_AUX_FAIL___20050101T000000_20500101T000000_300_004_3.EEF
SM_OPER_AUX_GALAXY_20050101T000000_20500101T000000_300_004_3
SM_OPER_AUX_GALNIR_20050101T000000_20500101T000000_300_003_3
SM_OPER_AUX_LSMASK_20050101T000000_20500101T000000_300_003_3
SM_OPER_AUX_MASK___20050101T000000_20500101T000000_300_002_3
SM_OPER_AUX_MISP___20050101T000000_20500101T000000_300_004_3.EEF
SM_OPER_AUX_MOONT__20050101T000000_20500101T000000_300_002_3
SM_OPER_AUX_RFI____20050101T000000_20500101T000000_300_003_3
SM_OPER_AUX_SUNT___20050101T000000_20500101T000000_300_002_3
SM_OPER_MIR_GMATD__20100101T144504_20100101T162500_600_007_3
SM_OPER_MIR_JMATD__20100101T144504_20100101T162500_600_007_3
SM_OPER_MPL_ORBSCT_20091102T031142_20500101T000000_401_001_1.EEF
SM_REPR_AUX_RFILST_20110101T000000_20110131T235959_100_016_3.EEF
SM_REPR_AUX_RFILST_20110501T000000_20110531T235959_100_016_3.EEF
SM_REPR_AUX_RFILST_20120701T000000_20120731T235959_100_016_3.EEF
SM_REPR_AUX_VTEC_C_20110127T230000_20110129T010000_311_001_3
SM_REPR_AUX_VTEC_C_20110430T230000_20110502T010000_311_001_3
SM_REPR_AUX_VTEC_C_20110501T230000_20110503T010000_311_001_3
SM_REPR_AUX_VTEC_C_20120630T230000_20120702T010000_311_001_3
SM_REPR_AUX_VTEC_C_20120702T230000_20120704T010000_311_001_3
SM_TEST_AUX_CNFL1P_20050101T000000_20500101T000000_720_001_0.EEF
SM_TEST_AUX_FRSNEL_20050101T000000_20500101T000000_720_001_0
SM_TEST_AUX_LCF____20050101T000000_20500101T000000_720_001_0.EEF
SM_TEST_AUX_NIR____20050101T000000_20500101T000000_720_001_0.EEF
SM_TEST_AUX_PATT___20050101T000000_20500101T000000_720_001_0
SM_TEST_AUX_PLM____20050101T000000_20500101T000000_700_002_0.EEF
SM_TEST_AUX_PMS____20050101T000000_20500101T000000_711_002_0.EEF
SM_TEST_AUX_SPAR___20050101T000000_20100111T120700_340_013_0.EEF
SM_TEST_AUX_SPAR___20100111T120700_20110112T091500_340_014_0.EEF
SM_TEST_AUX_SPAR___20110112T091500_20500101T000000_340_015_0.EEF
SM_TEST_MIR_AFWD1A_20100202T144510_20100202T162359_600_002_0
SM_TEST_MIR_GMATD__20100101T144504_20100101T162500_700_001_3
SM_TEST_MIR_JMATD__20100101T144504_20100101T162500_700_001_3
```